Cell Reports

Article

Synaptic vesicle binding of α-synuclein is modulated by β- and γ-synucleins

Graphical abstract

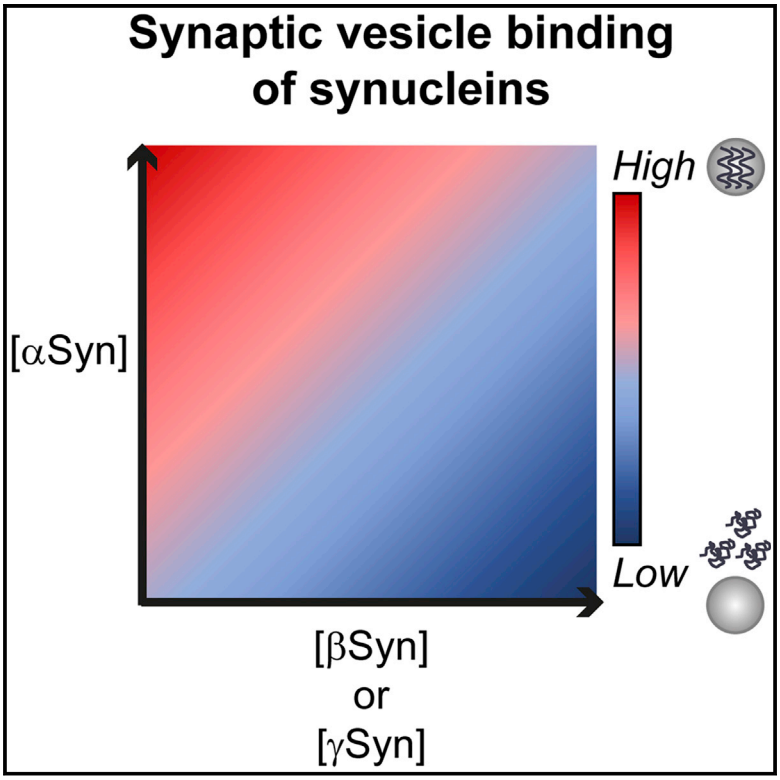

Highlights

- β- and γ-synuclein have a reduced membrane affinity compared with α-synuclein
- β- and γ-synuclein form heteromultimers with α-synuclein
- Synuclein heteromerization reduces synaptic vesicle binding of α-synuclein

Authors

Kathryn E. Carnazza, Lauren E. Komer, Ying Xue Xie, ..., David Eliezer, Manu Sharma, Jacqueline Burré

Correspondence

jab2058@med.cornell.edu

In brief

α-synuclein functions in synaptic neurotransmitter release by binding to synaptic vesicles. The roles of β- and γ-synuclein in this process are unknown. Carnazza et al. demonstrate that on the synaptic vesicle surface, synucleins form heteromultimers whose composition dictates the amount of physiologically active α-synuclein on synaptic vesicles.

Carnazza et al., 2022, Cell Reports *39*, 110675
April 12, 2022
https://doi.org/10.1016/j.celrep.2022.110675

CellPress

Cell Reports

CellPress
OPEN ACCESS

Article

Synaptic vesicle binding of α-synuclein is modulated by β- and γ-synucleins

Kathryn E. Carnazza,[1,5] Lauren E. Komer,[1,5] Ying Xue Xie,[1] André Pineda,[1] Juan Antonio Briano,[1] Virginia Gao,[1] Yoonmi Na,[1] Trudy Ramlall,[2] Vladimir L. Buchman,[3,4] David Eliezer,[2] Manu Sharma,[1] and Jacqueline Burré[1,6,*]

[1]Helen and Robert Appel Alzheimer's Disease Research Institute, Brain and Mind Research Institute, Weill Cornell Medicine, New York, NY 10021, USA

[2]Department of Biochemistry, Weill Cornell Medicine, New York, NY 10021, USA

[3]School of Biosciences, Cardiff University, Cardiff CF103AX, UK

[4]Belgorod State National Research University, 85 Pobedy Street, Belgorod, Belgorod 308015, Russian Federation

[5]These authors contributed equally

[6]Lead contact

*Correspondence: jab2058@med.cornell.edu

https://doi.org/10.1016/j.celrep.2022.110675

SUMMARY

α-synuclein, β-synuclein, and γ-synuclein are abundantly expressed proteins in the vertebrate nervous system. α-synuclein functions in neurotransmitter release by binding to and clustering synaptic vesicles and chaperoning SNARE-complex assembly. Pathologically, aggregates originating from soluble pools of α-synuclein are deposited into Lewy bodies in Parkinson's disease and related synucleinopathies. The functions of β-synuclein and γ-synuclein in presynaptic terminals remain poorly studied. Using *in vitro* liposome binding studies, circular dichroism spectroscopy, immunoprecipitation, and fluorescence resonance energy transfer (FRET) experiments on isolated synaptic vesicles in combination with subcellular fractionation of brains from synuclein mouse models, we show that β-synuclein and γ-synuclein have a reduced affinity toward synaptic vesicles compared with α-synuclein, and that heteromerization of β-synuclein or γ-synuclein with α-synuclein results in reduced synaptic vesicle binding of α-synuclein in a concentration-dependent manner. Our data suggest that β-synuclein and γ-synuclein are modulators of synaptic vesicle binding of α-synuclein and thereby reduce α-synuclein's physiological activity at the neuronal synapse.

INTRODUCTION

α-synuclein (αSyn), β-synuclein (βSyn), and γ-synuclein (γSyn) are abundantly expressed proteins in the vertebrate nervous system (Buchman et al., 1998b; George, 2002; Jakes et al., 1994; Ji et al., 1997; Lavedan et al., 1998; Nakajo et al., 1993). αSyn plays an important physiological role at the synapse, where it maintains neurotransmitter release by regulating synaptic vesicle pools (Cabin et al., 2002; Murphy et al., 2000; Yavich et al., 2004) and chaperoning SNARE-complex assembly (Burré et al., 2010). It exists in a synaptic-vesicle-bound α-helical state and a soluble, natively unfolded state in the cytosol, exchanging between these two pools in a dynamic equilibrium (Iwai et al., 1995; Kahle et al., 2000; Maroteaux et al., 1988). Pathologically, αSyn is a major component of Lewy bodies and Lewy neurites in Parkinson's disease (PD), Lewy body dementia, and related synucleinopathies (Arawaka et al., 1998; Gai et al., 1998; Spillantini et al., 1997; Wakabayashi et al., 1997). Neuropathology in synucleinopathies is proposed to originate from a toxic gain of function of αSyn aggregates. The soluble pool of αSyn spontaneously forms aggregates at a low rate, and this rate is increased with increased αSyn levels (Conway et al., 1998; El-Agnaf et al., 1998; Ibanez et al., 2004; Rochet et al., 2000; Singleton et al., 2003), and increased expression of αSyn correlates with PD risk, age of onset, and pathology in monkeys and humans (Chiba-Falek and Nussbaum, 2003; Chu and Kordower, 2007; Cronin et al., 2009; Linnertz et al., 2009; Maraganore et al., 2006). In addition, the inability of αSyn to bind to synaptic vesicle membranes increases its aggregation *in vitro* and triggers earlier neurotoxicity and pathology in mice, while membrane binding protects αSyn from aggregation (Burré et al., 2015). This suggests that an enlarged cytosolic pool of αSyn constitutes a risk factor for PD pathogenesis, and shifting αSyn from one pool to another may provide a mechanism for therapeutic strategies in synucleinopathies.

Despite the involvement of βSyn and γSyn in neurodegenerative diseases such as Lewy body dementia, diffuse Lewy body disease, motor neuron disease, neurodegeneration with brain iron accumulation type 1, glaucoma, and PD (Galvin et al., 1999, 2000; Nguyen et al., 2011; Ninkina et al., 2009; Nishioka et al., 2010; Peters et al., 2012; Surgucheva et al., 2002), virtually nothing is known about their physiological functions in the brain. βSyn has been suggested to be a regulator of cell survival (da Costa et al., 2003; Hashimoto et al., 2004), to decrease aggregation of αSyn (Brown et al., 2016; Hashimoto et al., 2001; Park and Lansbury, 2003; Uversky et al., 2002; Windisch et al., 2002), and

to be involved in dopamine handling (Ninkina et al., 2021). γSyn has been linked to several metastatic cancers, and proposed functions such as modulation of microtubules and chaperone activities have primarily been studied in an oncological context (Jiang et al., 2004; Zhang et al., 2011), although effects of γSyn on the neurofilament network and a chaperone-like activity have been demonstrated in cultured mouse neurons and photoreceptor cells, respectively (Buchman et al., 1998a; Surgucheva et al., 2005). Similar to αSyn, βSyn and γSyn both bind to and curve lipid membranes, and all synucleins are involved in regulating synaptic vesicle endocytosis (Sung and Eliezer, 2006; Vargas et al., 2014; Westphal and Chandra, 2013). In contrast to αSyn, γSyn does not bind to synaptobrevin-2 and does not affect SNARE-complex assembly (Ninkina et al., 2012). The effect of βSyn on SNARE complexes is unclear, and vesicle clustering has not been tested for βSyn or γSyn.

The three synucleins share a high degree of sequence homology (Jakes et al., 1994; Nakajo et al., 1993), have high gene and protein expression in the human brain, and show an overall similar regional distribution, but with several exceptions and differences in relative ratios (Ahmad et al., 2007; Buchman et al., 1998b; George, 2002; Iwai et al., 1995; Jakes et al., 1994; Jakowec et al., 2001; Jeannotte et al., 2009; Ji et al., 1997; Lavedan, 1998; Lavedan et al., 1998; Maroteaux and Scheller, 1991; Murphy et al., 2000; Ninkina et al., 1998; Ueda et al., 1993, 1994). The differential expression levels and imperfect overlap of synuclein expression seem to suggest that the three family members have distinct and separate roles. In support of this theory, studies found no compensatory increase in αSyn or βSyn expression upon knockout of γSyn (Ninkina et al., 2003; Papachroni et al., 2005), in βSyn upon knockout of αSyn and γSyn (Papachroni et al., 2005), or in βSyn or γSyn upon αSyn knockout (Abeliovich et al., 2000; Kuhn et al., 2007; Schluter et al., 2003). Lack of compensation was also surmised from a lack of exaggeration of phenotypes in α/γ-Syn double-knockout (KO) mice compared with αSyn and γSyn single-KO mice (Robertson et al., 2004). Redundancy was countered by a lack of potentiation of gene expression in α/γ-Syn-KO versus αSyn and γSyn single-KO mice (Kuhn et al., 2007); a reduction in striatal dopamine and specific protein levels in αSyn-null but not γSyn-null mice (Al-Wandi et al., 2010); a lack of γSyn ability to interact with VAMP2, support SNARE-complex assembly, and rescue the CSPα-KO phenotype (Ninkina et al., 2012); and a distinct effect of the lack of only βSyn in an inverted grid test as well as a distinct effect of the lack of only αSyn on striatal dopamine levels that was not exacerbated by additional loss of the other synucleins (Connor-Robson et al., 2016).

In contrast, in other studies, a compensatory function of βSyn and γSyn is supported by increased expression of the remaining family member in the CNS of α/β-Syn and α/γ-Syn double-KO mice (Chandra et al., 2004; Robertson et al., 2004) and accelerated pathology in CSPα-KO mice in the absence of both αSyn and βSyn compared with αSyn only (Chandra et al., 2005). Functional redundancy is supported by behavioral and dopamine release phenotypes in α/γ-Syn-KO mice, while single αSyn-KO or γSyn-KO mice showed no deficits (Senior et al., 2008), by considerable functional overlap in the pools of genes whose expression is changed in the absence of αSyn or γSyn (Kuhn et al., 2007) and by a decrease in dopamine levels in brains of α/β-Syn KO but not αSyn or βSyn single KO (Chandra et al., 2004). However, none of these studies have investigated functional redundancy at the molecular level. These discrepancies may be due to the fact that different brain regions and different animal ages were analyzed in these studies, or they may point to a different role of the three synucleins in the same cellular process.

Here, we identify an important physiological role for βSyn and γSyn at the molecular level that can explain and consolidate the findings above. Our data support a model in which all synuclein family members affect synapse function, but their specific roles in that process differ. In this model, only αSyn mediates the downstream function of vesicle clustering and SNARE-complex assembly, while βSyn and γSyn indirectly affect synapse function by modulating the binding of αSyn to synaptic vesicles. Our data suggest that shifting the equilibrium between the two intracellular pools of αSyn by modulating βSyn and/or γSyn may be a promising avenue for reducing αSyn aggregation, neurotoxicity, and pathology.

RESULTS

βSyn and γSyn reveal reduced ability to bind to membranes compared with αSyn

αSyn binds to synaptic vesicle membranes (Iwai et al., 1995; Kahle et al., 2000; Maroteaux et al., 1988), reflecting its preference for membranes with high curvature and small diameter (Davidson et al., 1998; Middleton and Rhoades, 2010). βSyn and γSyn share the highly conserved α-helical lipid binding motif, consisting of six or seven 11-mer repeats, with αSyn (Figure S1A) and can adopt the same two-helix conformation (Rivers et al., 2008; Sung and Eliezer, 2006), suggesting that they bind to lipids as well. However, the lipid binding domain of βSyn shares only 87% sequence identity with αSyn and lacks 11 residues toward the end, and γSyn shares only 68% sequence identity in the lipid binding domain (Figure S1A). Furthermore, when analyzing the α-helical domains of the synucleins in a helical wheel plot, several intriguing differences become apparent. First, αSyn reveals the most electrostatic interactions at the synuclein-phospholipid membrane interface (11 lysine residues), βSyn the fewest (9 lysine residues), and γSyn an intermediate number (10 lysine residues; Figure S1B). Second, αSyn and γSyn have seven 11-mer repeats, while βSyn has only six (Figures S1A and S1B). Third, γSyn reveals an increased number of hydrophilic residues within the membrane binding domain (Figure S1B), and fourth, βSyn has a reduced number of hydrophobic residues within the membrane binding area (Figure S1B). These differences may lead to different membrane binding properties.

Previous *in silico* and *in vitro* studies have reported on certain aspects of membrane binding of the synucleins (Bertoncini et al., 2007; Brown et al., 2016; Ducas and Rhoades, 2012; Middleton and Rhoades, 2010; Rao et al., 2009; Sharma et al., 2020; Sung and Eliezer, 2006). Yet, the three synucleins were never compared side by side in a systematic manner, and the *in vivo* relevance of the findings in the above studies remains unknown. We thus directly compared the abilities of αSyn, βSyn, and γSyn to bind to liposomes *in vitro* and to brain cell membranes *in vivo*.

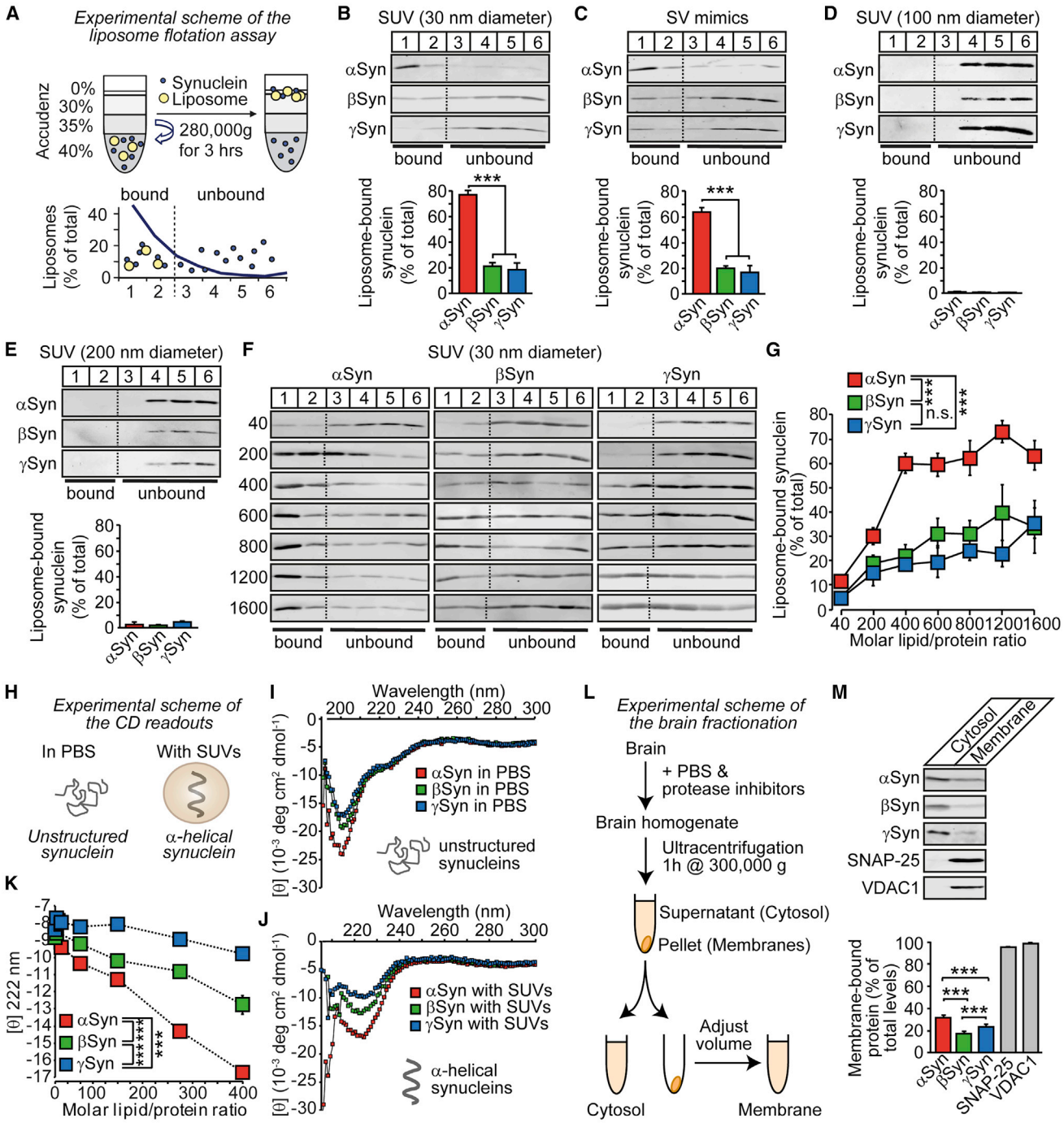

Figure 1. βSyn and γSyn reveal reduced ability to bind to membranes compared with αSyn

(A) Experimental scheme of the liposome binding assay. Liposomes mixed with synuclein were floated by density gradient centrifugation. Based on the liposome distribution in the gradient, assessed by a fluorescent lipid analog, the top two fractions 1 and 2 were defined as lipid-bound fractions.

(B–E) Binding of αSyn, βSyn, or γSyn to artificial small unilamellar vesicles (SUVs; composition: 70% L-α-phosphatidylcholine [PC], 30% L-α-phosphatidylserine [PS]) of 30 nm diameter (B), 100 nm diameter (D), or 200 nm diameter (E) or to synaptic vesicle mimics (30 nm diameter; composition: 36% PC, 30% L-α-phosphatidylethanolamine [PE], 12% PS, 5% L-α-phosphatidylinositol [PI], 7% sphingomyelin [SM], 10% cholesterol) (C). Binding was quantified as the sum of the top two fractions, plotted as the percentage of total synuclein in the gradient.

(F and G) Same as in (B), except that different molar lipid/protein ratios were used.

Data are means ± SEM (***$p < 0.001$ by Student's t test in B–E and two-way ANOVA in G; n = 6–8 independent experiments). See also Figure S1.

(legend continued on next page)

To assess membrane binding of the synucleins, we used a liposome flotation assay (Figure 1A). We first analyzed the ability of αSyn, βSyn, or γSyn to associate with liposomes of high curvature (~30 nm diameter), mimicking synaptic vesicles (Figures 1B and 1C). We found robust binding of αSyn to liposomes composed of 30% phosphatidylserine and 70% phosphatidylcholine (Figure 1B), as well as to liposomes mimicking the synaptic vesicle composition (Takamori et al., 2006) (Figure 1C). Strikingly, βSyn and γSyn revealed a dramatically reduced binding to both of these liposomes, which was not affected by deletion of the C termini, which are not important for the interaction with membranes (Figures 1B, 1C, and S1C).

While αSyn preferentially associates with liposomes of high curvature (Davidson et al., 1998; Middleton and Rhoades, 2010), βSyn and γSyn may have a preference for less curved membranes. We thus repeated our flotation assay in the presence of liposomes of 100 (Figure 1D) or 200 nm (Figure 1E) diameter, but lost binding of all synucleins to these larger liposomes.

Alternatively, αSyn, βSyn, and γSyn may have different affinities for lipids and thus potentially saturate at different liposome concentrations. We therefore tested binding of the synucleins to liposomes at different molar lipid/protein ratios, including ratios beyond the known saturation levels for αSyn (lipid/protein ratio of 300:1 to 400:1) (Chandra et al., 2003; Rocha et al., 2019) (Figures 1F and 1G). While we found saturation of binding for all synucleins around a molar lipid/protein ratio of 200:1 to 400:1, strikingly, βSyn and γSyn binding plateaued at a significantly lower liposome-bound protein percentage compared with αSyn (Figures 1F and 1G).

As a separate means to assess binding of synucleins to liposomes, we used circular dichroism (CD) spectroscopy. αSyn is natively unstructured in solution, but adopts an α-helical conformation upon binding to membranes (Davidson et al., 1998) (Figure 1H). While all synucleins had a similar unfolded nature in solution (Figure 1I), βSyn and γSyn had reduced α helicity at all molar lipid/protein ratios tested in comparison with αSyn (Figures 1J and 1K), with γSyn showing the lowest and βSyn intermediate levels of α-helical folding, supporting our liposome flotation data (Figures 1A–1G and S1).

The flotation and CD experiments above used purified recombinant synucleins and phospho-liposomes. To probe for membrane binding in a more physiological context, we performed subcellular fractionation on wild-type (WT) mouse brains to separate brain homogenates into cytosolic and membrane-bound fractions (Figure 1L). We found the integral membrane protein VDAC1 and membrane-associated protein SNAP-25 to be robustly associated with membrane fractions, demonstrating successful fractionation (Figure 1M). Synucleins were more cytosolic, reflecting their on/off membrane equilibrium, particularly when subjected to tissue homogenization. When we compared the membrane association of βSyn and γSyn with that of αSyn, we found a significant reduction in membrane-bound βSyn and γSyn, with αSyn > γSyn > βSyn detected in the membrane-bound fraction (Figure 1M). Importantly, our antibodies reveal no cross-reactivity among the synuclein family members or other proteins (Figure S2).

Overall, our data suggest a reduced ability of both βSyn and γSyn to associate with artificial phospholipid membranes as well as cellular brain membranes, compared with αSyn.

Reduced presynaptic localization of γSyn but not βSyn compared with αSyn

αSyn targets to presynaptic terminals by binding to synaptic vesicle membranes (Iwai et al., 1995; Kahle et al., 2000; Maroteaux et al., 1988) and to the synaptic vesicle protein synaptobrevin-2/VAMP2 (Burré et al., 2010, 2012). Subcellular compartment-specific membrane and/or protein interactions may thus affect the synaptic localization of all synucleins. We therefore enriched for synaptosomes from brain homogenates of WT mice using subcellular fractionation (Figure 2A) (Burré et al., 2006) and analyzed relative protein levels in synaptosomes compared with whole brain (Figures 2B and 2C). We found an ~2-fold enrichment for the synaptic vesicle protein synaptobrevin-2 in the synaptosome fraction, while the axonal/dendritic proteins α-tubulin and neurofilament of 165 kDa were depleted (Figures 2B and 2C), demonstrating successful synaptosome enrichment. When we analyzed the synucleins, we found neither enrichment nor depletion of αSyn and βSyn in WT synaptosomes compared with brain homogenates, while γSyn showed a significant depletion (Figures 2B and 2C).

Independently, we analyzed the synaptic co-localization of αSyn, βSyn, or γSyn with cytosolic, dendritic, or synaptic markers in cortical WT mouse neurons through immunocytochemistry (Figures 2D–2F and S2). We first assessed the relative intracellular localization using co-staining of the three synucleins with MAP2 and lentivirally transduced neuron-targeted TdTomato, revealing a punctate staining for αSyn and βSyn that was significantly less prominent for γSyn (Figures 2D, 2J, and S2F). We then analyzed the synaptic localization of synucleins, quantifying co-localization with the synaptic vesicle proteins synapsin, synaptobrevin-2, and SV2. We found a robust synaptic localization for αSyn and βSyn, similar to the integral synaptic vesicle proteins SV2 and synaptobrevin-2, while γSyn was not as synaptic (Figures 2E, 2F, 2H–2J, S2F, and S2G). Because γSyn is not as abundant as the other synucleins in the cortex, we repeated our analysis of γSyn localization in cultured midbrain neurons that have higher expression of γSyn (Figure S2H). We confirmed the more diffuse distribution within the neuronal cytoplasm and less profound synaptic localization for γSyn (Figure S2I).

(H–J) CD spectroscopy of synucleins. Experimental scheme of the CD readouts of αSyn as unstructured or α helical (H). Secondary structure of recombinant αSyn, βSyn, or γSyn in the absence (I) or presence (J) of 30 nm charged SUVs at a molar lipid/protein ratio of 400.

(K) Same as (J), except that different molar lipid/protein ratios were used, and the signal at 222 nm was plotted to highlight α helicity (***$p < 0.001$ by two-way ANOVA, mean of n = 3).

(L and M) *In vivo* membrane binding of synucleins. P30 WT brain homogenates were subjected to subcellular fractionation to yield cytosolic and membrane fractions (L). Equal volumes of protein were analyzed by quantitative immunoblotting (M). Data are means ± SEM (***$p < 0.001$ by Student's t test; n = 4 brains). See also Figure S2.

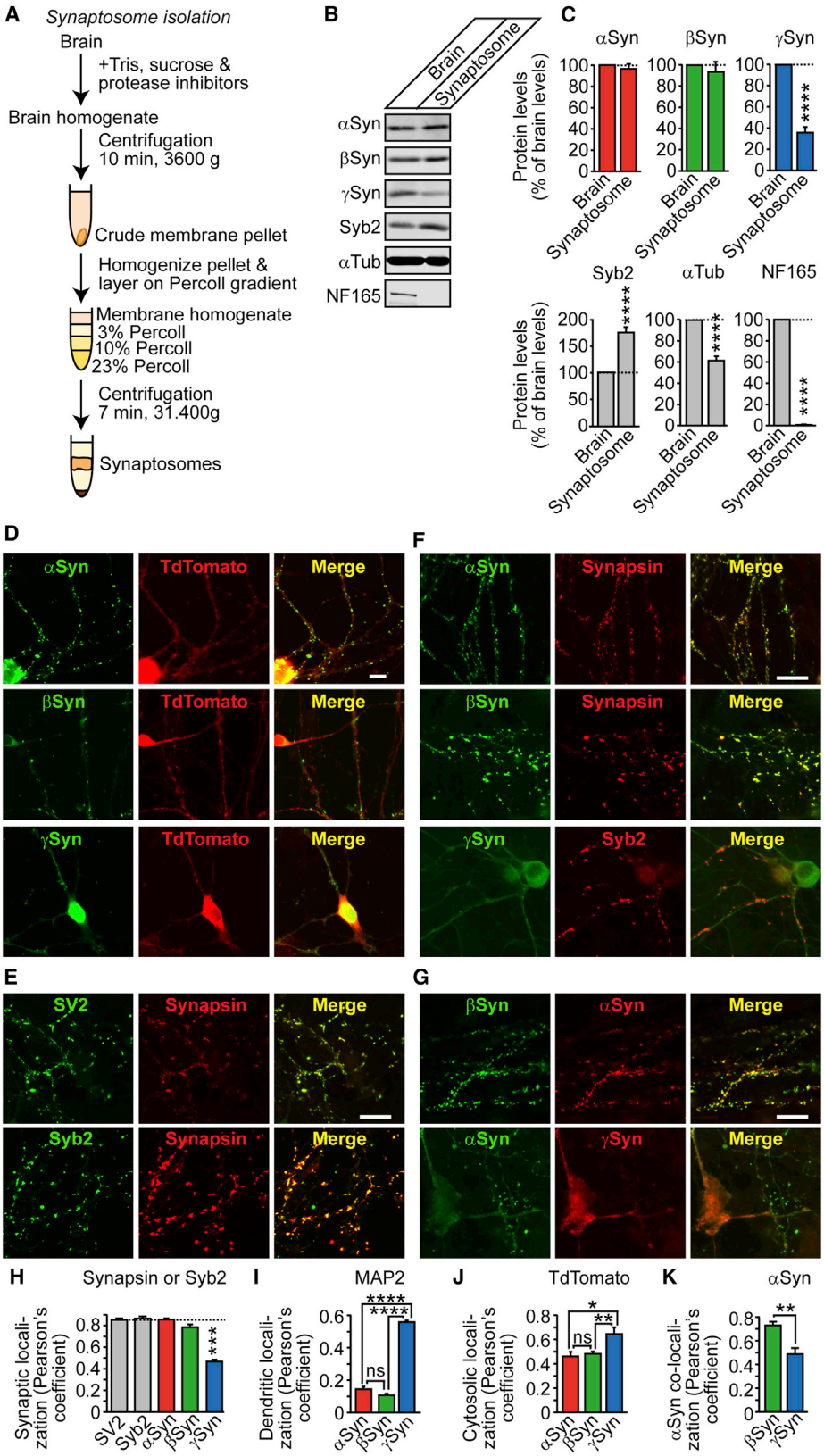

(legend on next page)

We also analyzed the co-localization of αSyn with either βSyn or γSyn and found robust co-staining of αSyn with βSyn, while the co-localization of αSyn with γSyn was less prominent (Figures 2G, 2K, and S2I). These findings indicate a potential for direct interaction among the synuclein family members.

Note that the readouts of the two assays above differ: during subcellular fractionation, brain tissue is subjected to several rounds of homogenization, which may result in a different on/off equilibrium of the synucleins. In addition, this biochemical procedure does not purify synaptosomes, but merely enriches for them. In contrast, the immunocytochemistry experiments instantaneously fix the position of synucleins and focus only on overlap at the presynaptic terminal. Thus, relative enrichment of proteins in these two assays differs.

Synucleins interact with one another in a specific conformation

βSyn and, to a lesser extent, γSyn, still target to the synapse, despite having a dramatically reduced ability to associate with membranes compared with αSyn. What is the underlying mechanism for this? Based on our previous studies showing homomultimerization of the membrane binding domain of αSyn (Burré et al., 2014), we hypothesized that synucleins may interact with one another, thereby potentially enabling synaptic localization of βSyn and γSyn despite their own low affinity for membranes (Figures 1 and 2). There is supporting evidence for synuclein interfamily interactions, including α/β-Syn heterodimers and weak to moderate micromolar binding affinities between all family members (Jain et al., 2018; Janowska et al., 2015; Sanjeev et al., 2017; Tsigelny et al., 2007), but these studies are all *in silico* or *in vitro* or use overexpression in yeast, so their physiological relevance remains unclear.

When we probed for interactions among the synucleins using co-immunoprecipitation in the presence of detergent, and thus the absence of membranous structures, we did not detect any binding (Figures S3A and S3B), unlike the *in vitro* studies mentioned above. Given that dimers and higher-order multimers of αSyn form only upon membrane binding of αSyn and not in solution (Burré et al., 2014), αSyn-βSyn and αSyn-γSyn interactions may require membranes as well. We therefore adapted a fluorescence resonance energy transfer (FRET) system that we had previously used to assess the specific configuration of αSyn multimers on membranes (Burré et al., 2014). For this, we introduced cysteine residues at the beginning and the end of the α-helical domains of the synucleins (Figure 3A), generated recombinant proteins, and labeled these cysteines with either Alexa 488 or Alexa 546 (Figure 3B). Based on our previous studies (Burré et al., 2014), we hypothesized that not only homomultimers, but also heteromultimers, of synucleins would adopt the antiparallel broken helix configuration, and thus, we labeled only residues within the synucleins that match this configuration (Figures 3A and 3B). We ensured that the labeling efficiency was comparable between the different synuclein variants, by comparing the donor and acceptor fluorescence emissions (Figures S3C–S3J) and by direct measurement of the labeling efficiency (Figure S3K). We then measured FRET between various synuclein combinations, including both inter- and intrafamily combinations, in the presence of 30 nm diameter charged liposomes (Figures 3C), 100 nm diameter charged liposomes (Figure 3D), or 30 nm diameter neutral liposomes (Figure 3E). Only in the presence of 30 nm charged liposomes did we detect an FRET signal between αSyn, βSyn, or γSyn, suggesting that all synucleins share the ability to form homodimers in a specific conformation (Figures 3F and S4A–S4C). As expected, we were unable to detect any FRET signal between synucleins in the presence of 30 nm neutral liposomes or in the presence of 100 nm charged liposomes, which synucleins do not bind to very well (Figures 1, 3D–3F, and S4A–S4C).

We then tested for the ability of synucleins to form heteromultimers. Similar to the intrafamily FRET results (Figure 3F), all synucleins demonstrated the ability to interact with one another in the presence of 30 nm charged but not 30 nm neutral or 100 nm charged liposomes (Figures 3G and S4D–S4F).

βSyn and γSyn reduce synaptic targeting of αSyn in a dose-dependent manner

Does this *in vitro* interaction among synucleins have a functional consequence *in vivo*? We had already established the co-expression of αSyn/βSyn and αSyn/γSyn within the same neuron and within synaptic compartments (Figures 2G, 2K, and S2), although not all presynaptic terminals stained equally strong for each of the synucleins, indicating heterogeneity in synuclein levels in different neurons.

To test for a functional *in vivo* consequence, we first analyzed if the presence or absence of βSyn or γSyn results in changes in the synaptic targeting of αSyn. We transduced primary αβγ-Syn triple-KO neurons with a stable amount of lentivirus expressing αSyn and increasing amounts of lentivirus expressing either βSyn or γSyn (Figure 4A). Half of the wells were used for immunocytochemistry, the other half for immunoblotting. When we analyzed the levels of synucleins in these neurons, we found αSyn levels to be mostly stable and βSyn and γSyn levels to increase similarly with increasing virus amount (Figures 4B–4E). Note that not absolute levels but the relative αSyn/βSyn and αSyn/γSyn ratios matter the most for this readout.

Figure 2. Reduced presynaptic localization of γSyn but not βSyn compared with αSyn

(A–C) Synaptosome isolation. Experimental scheme (A). Enrichment analysis of proteins in synaptosomal preparations (B, C). Brains of P40 WT mice were homogenized and subjected to subcellular fractionation to yield synaptosomes. Twenty micrograms of brain homogenate and synaptosomes was analyzed by quantitative immunoblotting (Syb2, synaptobrevin-2; αTub, α-tubulin; NF165, neurofilament of 165 kDa). Data are means ± SEM (****p < 0.0001 by Student's t test; n = 4 brains).

(D–K) Synaptic targeting of synucleins. Cultured cortical WT mouse neurons were analyzed at 27 days *in vitro* for co-localization with the indicated proteins (D–G). Synapsin-promoter-driven expression of TdTomato (D) was achieved via lentiviral transduction. Co-localization was quantitated using Pearson's coefficient (H–K). Data are means ± SEM (*p < 0.05, **p < 0.01, ***p < 0.001, ****p < 0.0001 by Student's t test; n = 6 independent cultures). Scale bar, 10 μm.

See also Figure S2.

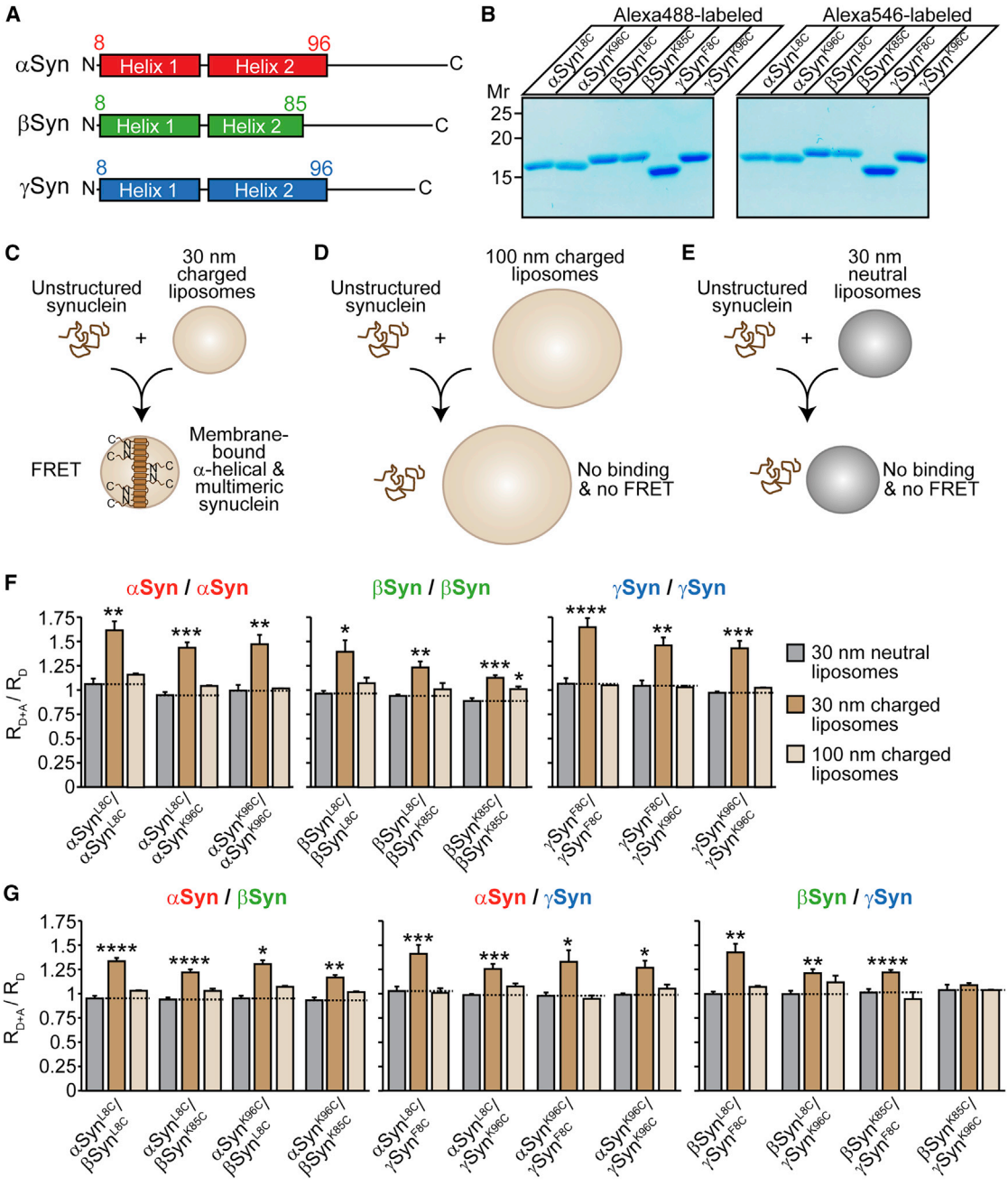

Figure 3. Synucleins interact with one another in a specific conformation

(A) Synuclein labeling scheme for FRET experiments. Single-cysteine substitutions were introduced into synucleins at positions 8 and 96 for αSyn and γSyn and at positions 8 and 85 for βSyn for modification with Alexa 488- or Alexa 546-maleimide.

(B) SDS-PAGE analysis of 5 μg purified Alexa 488- or Alexa 546-labeled recombinant αSyn.

(C–E) Experimental scheme for the FRET experiments in the presence of 30 nm diameter charged (C), 100 nm diameter charged (D), or 30 nm diameter neutral liposomes (E), with expected outcomes.

(F and G) Emission spectra in Figures S5 and S6 were used for calculation of FRET signals. Data are means ± SEM (*p < 0.05, **p < 0.01, ***p < 0.001, ****p < 0.0001 by Student's t test; n = 4–9 independent experiments). See also Figures S3 and S4.

We then quantified synaptic targeting of αSyn with increasing levels of βSyn or γSyn, measuring co-localization with the synaptic vesicle protein synapsin (Figures 4F–4H and S5A–S5D). We found a decrease in the synaptic localization of αSyn with increasing βSyn or γSyn levels, which was more prominent for βSyn (Figure 4I). Because a recent study reported that αSyn and synapsin interact (Atias et al., 2019), which may indirectly affect our results, we separately measured synaptic targeting

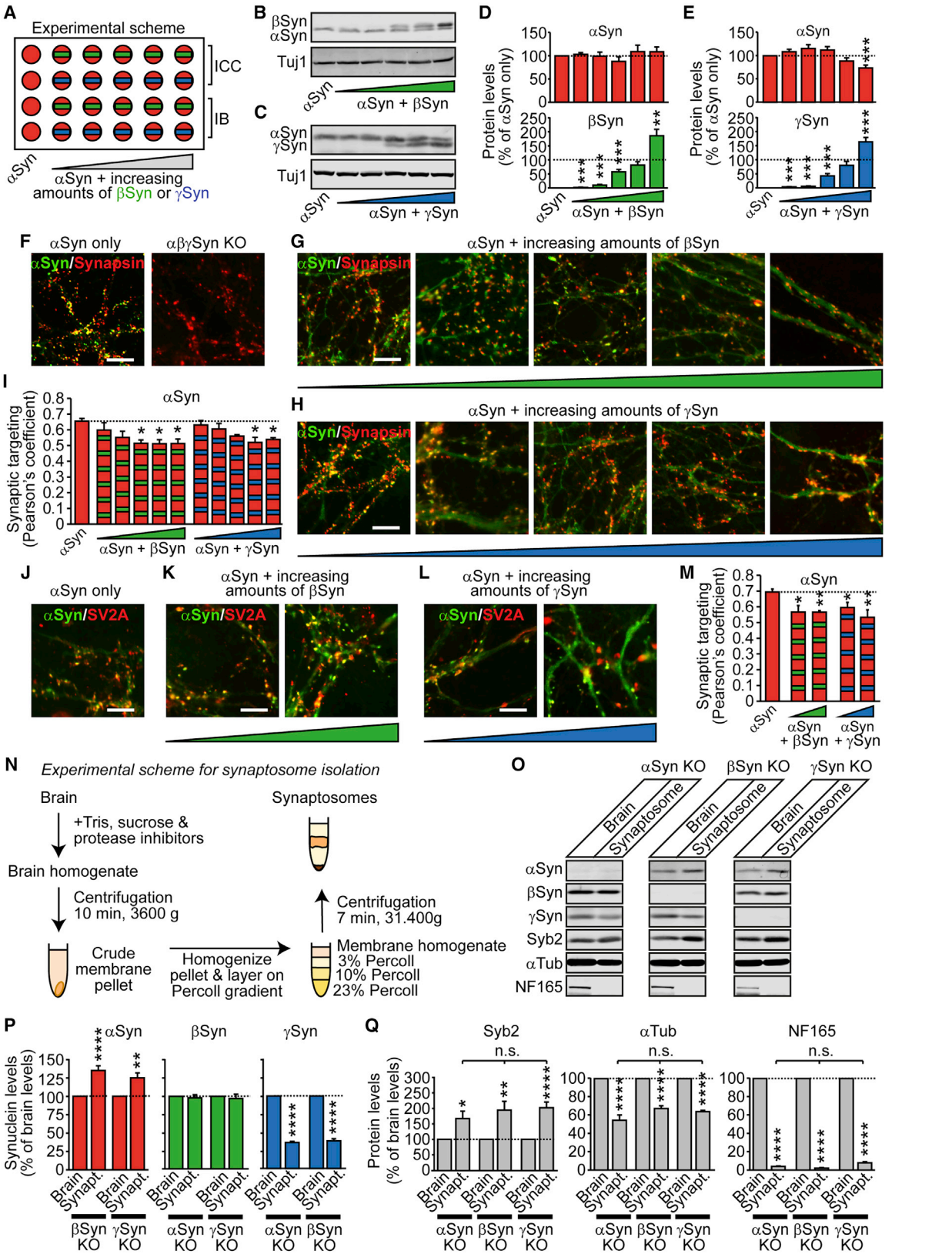

(legend on next page)

of αSyn by co-localization with the integral synaptic vesicle protein SV2. Again, we found a reduction in αSyn synaptic targeting with increasing expression of βSyn or γSyn (Figures 4J–4M and S5E–S5G).

To ensure that we were not saturating synaptic vesicles with these increasing amounts of synucleins, we performed the same titration experiments for αSyn (Figure S5H). Even with 2.5-fold increased αSyn levels (Figures S5I and S5J), we did not detect changes in the synaptic targeting of αSyn (Figures S5K–S5M).

While the above system is powerful, we wanted to ensure that our results were not confounded by overexpression of the viral transduction process, as overexpression may result in synuclein aggregation. We first assessed aggregation of αSyn in αβγ-Syn triple-KO neurons using lentiviral titrations, ranging from our standard concentration (1×) to 60-fold that amount. In parallel, we transfected neurons using calcium phosphate with 3, 6, 9, or 12 μg of a cytomegalovirus (CMV)-driven αSyn expression vector. We then stained the neurons for MAP2 and αSyn phosphorylated at S129, a marker of synuclein pathology (Anderson et al., 2006; Fujiwara et al., 2002). We failed to detect pS129-positive αSyn staining in our lentiviral transductions, even at 60-fold virus levels, and obtained staining similar for neurons that were not transduced (Figure S6A). In contrast, the CMV-driven αSyn transfection experiments resulted in robust pS129-positive αSyn foci, which increased in number and fluorescence intensity with increasing αSyn cDNA amount (Figure S6A). In parallel, we assessed levels of αSyn and βSyn at our normal lentiviral transduction levels compared with endogenous levels in WT neurons, using quantitative immunoblotting. The lentiviral expression constructs were myc-tagged, enabling direct comparison of endogenous and myc-tagged αSyn and βSyn (Figure S6B). We found no significant difference in expression of lentivirally expressed αSyn and βSyn compared with endogenous αSyn or βSyn (Figure S6B). Note that we were unable to perform a similar analysis for γSyn because our antibody detects only endogenous mouse γSyn and not the human γSyn produced by the lentiviral vector. Last, because small αSyn oligomers may not be apparent in the immunocytochemical analyses, we also assessed the potential aggregation of αSyn using immunoblotting of WT neuron cultures transduced with 10×, 20×, and 60× lentiviral amounts of what we usually use for our experiments. We found significant oligomerization only at 20× and 60× viral amounts and confirmed specificity of the oligomer signal using aggregated recombinant αSyn (Figure S6C).

Despite the lack of aggregation of αSyn in our system and the expression at endogenous levels, we additionally examined synaptic targeting at endogenous expression levels without lentiviral manipulation by generating single αSyn-, βSyn-, and γSyn-KO mice from our αβγ-Syn triple-KO mice. We first assessed if absence of any synuclein family member would lead to a compensatory change in another. This was, however, not the case (Figures S7A and S7B), enabling us to directly compare the three genotypes.

We then analyzed synaptic targeting of αSyn, βSyn, and γSyn using the synaptosome enrichment study we had previously performed for WT brains (Figures 2 and 4N). When we compared the relative amount of synucleins in synaptosomes versus total brain, we found significantly more synaptic αSyn in the absence of βSyn or γSyn (Figures 4O and 4P) compared with WT brains (Figures 2B and 2C). Importantly, this was not due to changes in the efficiency of subcellular fractionation, as synaptosomal enrichment of the synaptic vesicle protein synaptobrevin-2 and depletion of the cytoskeletal proteins α-tubulin and NF165 were identical among the genotypes and compared with WT brains (Figures 2, 4O, and 4Q).

Synucleins directly modulate one another's ability to associate with synaptic vesicles

Our data above suggest that the synaptic levels of αSyn are reduced with increasing levels of βSyn or γSyn, with βSyn having a slightly stronger effect than γSyn. These reductions could be mediated by a variety of factors, but we hypothesized that it may be due to direct binding of the synucleins. To test directly if βSyn and γSyn reduce the ability of αSyn to associate with synaptic vesicle membranes, we measured liposome binding of αSyn in the absence or presence of equal amounts of βSyn or γSyn and vice versa using a liposome flotation assay (Figure 5A). Interestingly, we found a significant reduction in membrane association of αSyn whenever βSyn or γSyn was present (Figure 5B). Conversely, we found an increase in membrane association of βSyn and γSyn whenever αSyn was present, with a slightly larger increase for γSyn compared with βSyn (Figures 5C and 5D). These findings, along with our FRET data

Figure 4. βSyn and γSyn reduce synaptic targeting of αSyn in a dose-dependent manner

(A) Experimental scheme of the βSyn and γSyn titration experiments. ICC, immunocytochemistry; IB, immunoblot.

(B–E) Analysis of synuclein levels. αβγ-Syn triple-knockout neurons were transduced with lentiviral vectors expressing αSyn only (A; 5 μL of 40× lentiviral particles) or constant αSyn levels (5 μL of 40× lentiviral particles) with increasing amounts of βSyn or γSyn (B–E; 0.2, 0.5, 1, 2, or 5 μL of 40× lentiviral particles). Data are means ± SEM (**$p < 0.01$, ***$p < 0.001$ by Student's t test; n = 11–12 independent cultures). All synucleins were myc-tagged, enabling direct comparison of their levels on the same blot using an antibody to myc.

(F–I) Synaptic targeting of αSyn. αβγ-Syn triple-knockout neurons were transduced as in (B)–(E). Synaptic targeting was quantified by co-localization with synapsin and Pearson's coefficient (I). Data are means ± SEM (*$p < 0.05$ by Student's t test; n = 3 cultures). Scale bar, 10 μm. See also Figures S5A–S5D.

(J–M) Same as in (F)–(I), except that co-localization of αSyn was assessed with SV2 in the presence of αSyn only (J, M; 5 μL of 40× lentiviral particles) or constant αSyn levels (5 μL of 40× lentiviral particles) with increasing amounts of βSyn or γSyn (K–M; 1 or 5 μL of 40× lentiviral particles). Data are means ± SEM (*$p < 0.05$, **$p < 0.01$ by Student's t test; n = 3 cultures). Scale bar, 10 μm. See also Figure S5.

(N–Q) αSyn enrichment in synaptosomes from mice of different genotypes. Synaptosomes were isolated from mouse brain homogenates of mice lacking αSyn, βSyn, or γSyn via subcellular fractionation (N; see Figures 2B and 2C for data obtained from WT mice), and 20 μg of homogenate and synaptosomes was analyzed by quantitative immunoblotting (Syb2, synaptobrevin-2; αTub, α-tubulin; NF165, neurofilament of 165 kDa; O–Q). Data are means ± SEM (*$p < 0.05$, **$p < 0.01$, ****$p < 0.0001$ by Student's t test; n.s., not significant; n = 6–8 mice).

See also Figure S7.

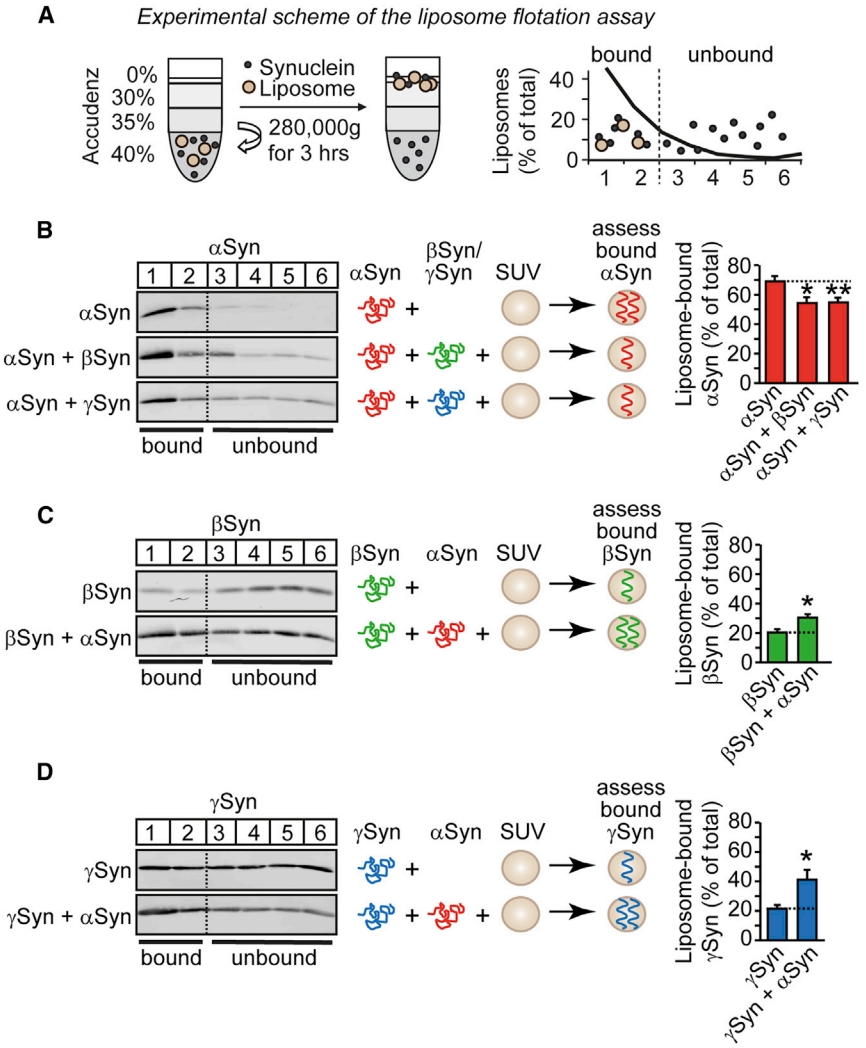

Figure 5. Synucleins directly modulate one another's ability to associate with membranes

(A) Experimental scheme of the liposome binding assay.

(B) Liposome binding of αSyn, quantified as the sum of the top two fractions as a percentage of total αSyn in the gradient, was analyzed in the absence or presence of equal amounts of βSyn or γSyn. Data are means ± SEM (*$p < 0.05$, **$p < 0.01$ by Student's t test; n = 6–15 independent experiments). Experiments with twice the amount of αSyn in αSyn-only flotations revealed results identical to the ones shown (data not shown).

(C and D) Liposome binding of βSyn (C) or γSyn (D) was analyzed in the absence or presence of equal amounts of αSyn by a flotation assay as in (B). Data are means ± SEM (*$p < 0.05$ by Student's t test; n = 6–15 independent experiments). Experiments with twice the amount of βSyn (C) or γSyn (D) in βSyn- or γSyn-only flotations revealed results identical to the ones shown above (data not shown).

(Figure 3), suggest that synucleins directly affect one another's ability to bind to synaptic vesicle membranes through direct synuclein-synuclein interaction.

Because liposomes lack the protein constituents of synaptic vesicles, which may affect binding of the synucleins, we next assessed binding of the synucleins to isolated synaptic vesicles. We first isolated synaptosomes by subcellular fractionation, osmotically lysed synaptosomes, and then fractionated synaptic vesicle pools using sucrose gradient centrifugation (Figure 6A). In this system, synaptic vesicles separate into a free synaptic vesicle pool devoid of markers for the plasma membrane or other organelles (fractions 5–11), while docked and active zone synaptic vesicles migrate to lower density fractions (fractions 23–31) (Burré et al., 2006; Morciano et al., 2005) (Figure 6B). We then immunoisolated synaptic vesicles from the free synaptic vesicle pool using an antibody to the synaptic vesicle protein SV2 and magnetic beads (Burré et al., 2006, 2007) and added recombinant synucleins labeled with Alexa 488 or Alexa 546 to assess FRET (Figure 6C). We found robust FRET for αSyn multimers on synaptic vesicles, while FRET for βSyn or γSyn multimers was significantly and similarly reduced (Figures 6D and 6G). When we assessed FRET for the heteromultimers αSyn/βSyn (Figure 6E) or αSyn/γSyn (Figure 6F), we found a reduction that was similar to the FRET signal obtained for βSyn or γSyn homomers alone (Figures 6D–6G), suggesting that βSyn and γSyn reduce synaptic vesicle binding of αSyn. In the absence of synaptic vesicles, no FRET was observed (Figures 6H and S7C–S7E), confirming that synuclein multimers form only in the presence of membranes.

Independently, and to better quantify the amount of synaptic-vesicle-bound synucleins, we immunocaptured free synaptic vesicles on magnetic beads, added equal molarity of recombinant synucleins either alone or in combination, and measured the amount of immunoprecipitated synucleins (Figure 6I). We found a significantly reduced binding for βSyn and γSyn compared with αSyn, with γSyn binding slightly better than βSyn (Figures 6J and 6K), mimicking our data on liposomes (Figure 1). When we assessed the effects of equal or 4-fold amounts of βSyn or γSyn on synaptic vesicle binding of αSyn, we found a dose-dependent reduction in αSyn binding, with γSyn having a stronger effect, while binding of βSyn or γSyn was only slightly stabilized in the presence of αSyn (Figures 6L–6N).

Overall, our data demonstrate that βSyn and γSyn have a reduced ability to associate with synaptic vesicle membranes compared with αSyn and reduced binding of αSyn to synaptic vesicles in a dose-dependent manner (Figure 7A), likely because of the reduced affinity of the αSyn/βSyn and αSyn/γSyn heteromers for the synaptic vesicle surface. We propose that synuclein heteromerization may provide a tuning mechanism for αSyn function in synaptic vesicle clustering and neurotransmitter

CellPress
OPEN ACCESS

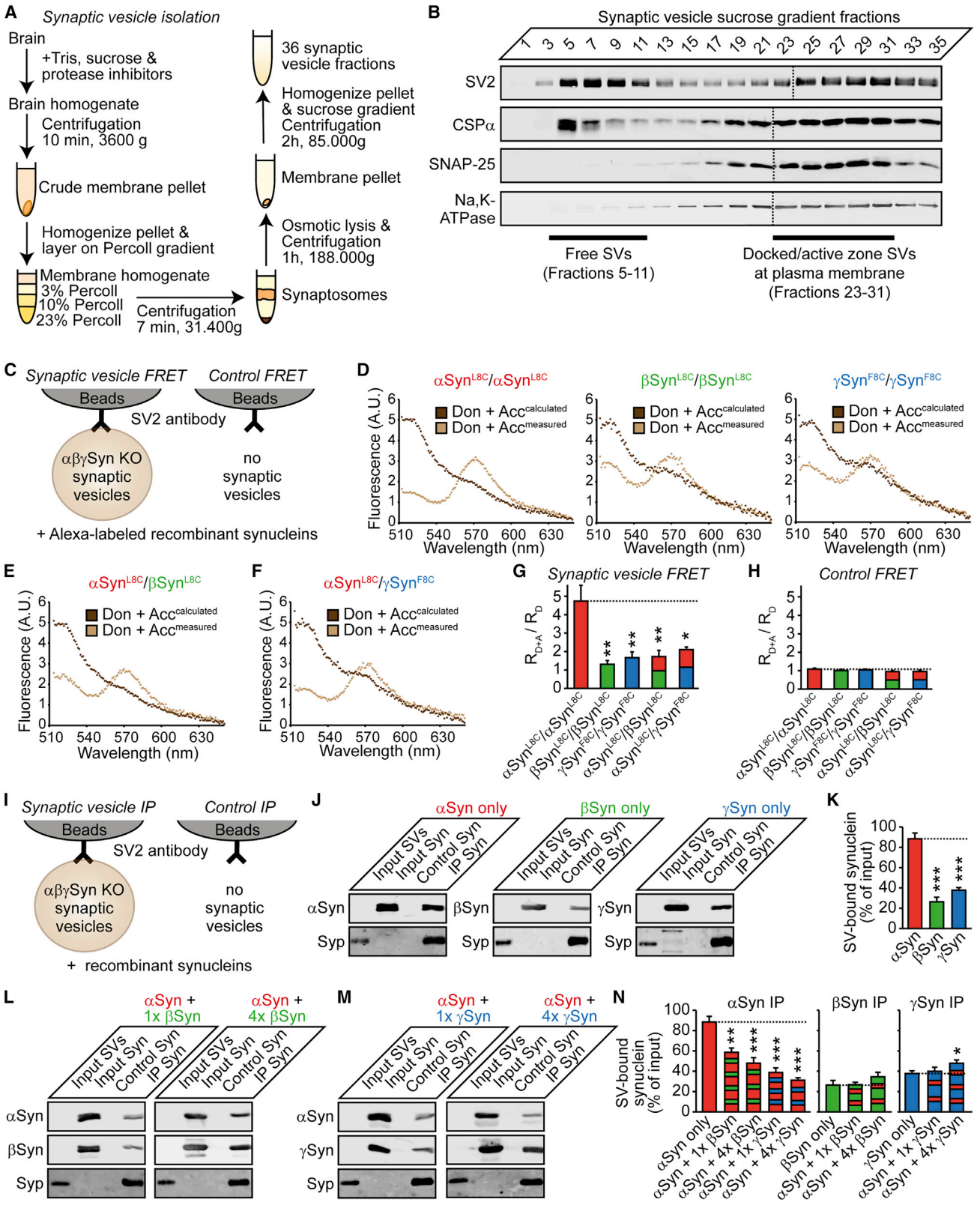

(legend on next page)

release, and may additionally provide therapeutic strategies to prevent αSyn aggregation and pathology (Figure 7B).

DISCUSSION

The function of αSyn is tightly linked to its localization in presynaptic terminals. Targeting of αSyn to terminals is mediated by binding to synaptic vesicle lipids and synaptobrevin-2 (Burré et al., 2010; Iwai et al., 1995; Kahle et al., 2000; Maroteaux et al., 1988; Sun et al., 2019). Binding of αSyn to synaptic vesicles triggers its multimerization which, in concert with binding of αSyn to synaptobrevin-2, promotes SNARE-complex assembly (Burré et al., 2010, 2014) and synaptic vesicle clustering (Diao et al., 2013; Sun et al., 2019). It has been suggested that this clustering activity restricts synaptic vesicle mobility between synapses to maintain recycling pool homeostasis (Scott and Roy, 2012) and helps regulate a reserve pool of synaptic vesicles for long-term operation of a neuron during high-frequency stimulation (Diao et al., 2013). In support of this theory, loss of synucleins increases tethering of synaptic vesicles to the active zone and reduces links between vesicles (Vargas et al., 2017), while interlocked αSyn/synaptobrevin-2 dimers reduce vesicle dispersion (Sun et al., 2019). In addition, Ca^{2+} and thus neuronal activity has been suggested to regulate the interaction of αSyn with synaptic vesicles (Lautenschlager et al., 2018), and electron microscopy studies show a redistribution of αSyn with activity (Atias et al., 2019; Tao-Cheng, 2006). In contrast, the physiological functions of βSyn and γSyn have remained largely elusive, although inhibition of αSyn aggregation by βSyn or γSyn has been proposed *in vitro* and in overexpression systems (Brown et al., 2016; Hashimoto et al., 2001; Park and Lansbury, 2003; Uversky et al., 2002; Van de Vondel et al., 2018; Windisch et al., 2002). Other studies have focused on possible synuclein interfamily interactions, but all of these studies were done *in vitro* or *in silico* and in the absence of membranes (Jain et al., 2018; Janowska et al., 2015; Sanjeev et al., 2017; Tsigelny et al., 2007), and no study has investigated the functional implications of these potential interactions at the molecular level.

Using biophysical, biochemical, and cell biological readouts in combination with mouse models, we have compared here side-by-side the ability of synucleins to (1) bind to synaptic vesicle membranes *in vitro* and *in vivo*, (2) target to the presynaptic terminal in the presence and absence of one another, (3) interact with one another in a specific conformation and membrane-dependent manner, and (4) modulate one another's ability to bind to synaptic vesicles. These findings suggest a control mechanism for synaptic vesicle binding of αSyn where both βSyn and γSyn reduce the amount of synaptic-vesicle-bound αSyn, and thereby shift the membrane-cytosol equilibrium of αSyn toward the non-functional and more aggregation-prone cytosolic pool (Figure 7). βSyn seems overall more potent *in vivo* compared with γSyn, likely because of its higher presence in synaptic terminals, while *in vitro*, the activity of γSyn is higher. This suggests that the intrinsic ability of γSyn to associate with membranes is higher compared with that of βSyn, but has a lower impact on synaptic vesicle binding of αSyn *in vivo* due to its lower representation in presynaptic terminals. By fine-tuning the amount of αSyn on synaptic vesicles, βSyn and γSyn have the ability to regulate αSyn function. These findings suggest that the molecular roles of synucleins are complementary but not functionally redundant, which may explain some of the conflicting and controversial findings in the field.

How is this process regulated within a presynaptic terminal where two or three synucleins co-localize? The decrease in αSyn interaction with the synaptic vesicle membrane could be due to direct competition of the synucleins for binding sites on the synaptic vesicle membrane. In addition, under conditions in which there are limited binding sites on the synaptic vesicle membrane for synuclein multimers, αSyn/βSyn or αSyn/γSyn heterodimerization would result in a quantitative reduction in the attachment of αSyn, without changing its affinity to synaptic vesicles. In these cases, more αSyn would bind to the vesicle surface in neurons lacking βSyn or γSyn due to lack of competition. However, βSyn and γSyn reveal a reduced binding affinity toward membranes and synaptic vesicles (Figures 1, 2, and 6) and increasing αSyn 2.5-fold does not affect synaptic targeting of αSyn (Figure S5), so unless there is an excess amount of βSyn or γSyn in a presynaptic terminal, competition is unlikely to be a significant factor. In support of this, a recent study evaluated the amounts of the three synucleins in synaptosomes isolated from whole rat brains using quantitative proteomics, and found similar levels of αSyn and βSyn, but around 6-fold less γSyn (Taoufiq et al., 2020), although this does not take into account potential differences in brain subregions or single neurons. The presence of αSyn also increases membrane binding of βSyn and γSyn (Figures 5C and 5D), which is an additional argument against competition. Alternatively, and supported by our data, binding of βSyn or γSyn to αSyn on the synaptic vesicle surface may reduce the affinity of αSyn for synaptic vesicle membranes through the formation of lower affinity αSyn/βSyn or αSyn/γSyn

Figure 6. Heteromerization of βSyn or γSyn with αSyn on synaptic vesicles reduces binding of αSyn

(A) Experimental scheme of the synaptic vesicle isolation procedure.

(B) Synaptic vesicles separate into two distinct populations on the sucrose gradient: a free synaptic vesicle (SV) pool devoid of plasma membrane markers and other organelles, and a pool that is docked to the plasma membrane and part of the active zone. The dotted lines indicate where blots were merged (note that fractions 23 and 25 were loaded on both gels to enable cross-membrane comparison).

(C–H) FRET experiments on synaptic vesicles. Synaptic vesicles were immunoisolated using magnetic beads and an antibody to the vesicle protein SV2 in the presence of Alexa-labeled recombinant synucleins, with beads lacking vesicles as controls (C). Upon washing, fluorescence spectra were recorded for the indicated FRET pairs (D–F; Don, donor; Acc, acceptor), and FRET was calculated in the presence (G) or absence (H) of synaptic vesicles. Data are means ± SEM (*p < 0.05, **p < 0.01 by Student's t test; n = 5–6 independent experiments). See also Figure S7.

(I–N) Immunoprecipitation experiments on synaptic vesicles. Synaptic vesicles were immunoisolated as in (C) in the presence of recombinant purified synucleins, with beads lacking synaptic vesicles as controls (I). Upon washing, the amount of bound αSyn, βSyn, or γSyn when incubated alone (J, K) or when 1- or 4-fold molar amounts of βSyn or γSyn were added (L, M) was quantified (N). Data are means ± SEM (*p < 0.05, **p < 0.01, ***p < 0.001 by Student's t test; n = 6 independent experiments).

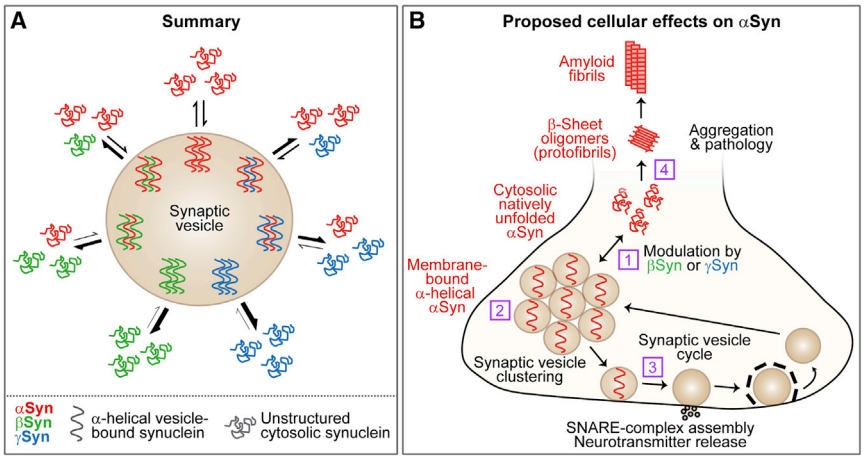

Figure 7. Summary of data and proposed model of the effect of βSyn or γSyn on αSyn

(A) Summary of our findings. Synucleins exist in a dynamic equilibrium between an α-helical, multimeric synaptic-vesicle-bound state and a natively unstructured cytosolic state. Different binding affinities of the synucleins for synaptic vesicles shift this equilibrium more toward synaptic vesicles or the cytosol, resulting in robust membrane binding of αSyn (red) and less robust binding of βSyn (green) and γSyn (blue), also indicated by arrow thicknesses. The binding of αSyn/βSyn or αSyn/γSyn heterodimers depends on the dose of βSyn and γSyn and shifts the equilibrium for αSyn more toward the cytosolic pool.

(B) Model of cellular effects of βSyn and γSyn on αSyn function and dysfunction. In the presynaptic terminal, αSyn cycles between a cytosolic and a synaptic-vesicle-bound pool (1). Binding to synaptic vesicles leads to synaptic vesicle clustering (2), which restricts synaptic vesicle mobility and thereby provides a reserve pool for long-term functioning of the nerve terminal. Via this process, αSyn promotes SNARE-complex assembly at the presynaptic plasma membrane and thereby affects neurotransmitter release (3). Via heteromultimerization, βSyn and γSyn reduce synaptic-vesicle-bound αSyn (1), which leads to a reduction in αSyn's physiological activities (2, 3). Rendering αSyn less membrane bound through the presence of βSyn and γSyn may increase the aggregation-prone cytosolic pool of αSyn (4) or, alternatively, binding of αSyn to βSyn or to γSyn may shield the aggregation-prone residues in αSyn, thereby also modifying αSyn-mediated pathology (4).

heteromers. Regardless of the specific mechanism, our findings raise several important questions that are essential for our understanding of synuclein biology and pathology and will need to be addressed in follow-up studies. These include, how much synaptic-vesicle-bound αSyn is necessary for αSyn to perform its role in synaptic vesicle clustering, SNARE-complex assembly, and neurotransmitter release? Are the significantly lower affinities of βSyn and γSyn sufficient to support their yet unknown functions on synaptic vesicles? What are the relative ratios of synucleins in different neurons, and do these have an impact on synapse function and strength?

The three synucleins are co-expressed at varied levels in the brain (Buchman et al., 1998b; George, 2002; Iwai et al., 1995; Jakes et al., 1994; Jakowec et al., 2001; Ji et al., 1997; Lavedan, 1998; Lavedan et al., 1998; Maroteaux and Scheller, 1991; Ueda et al., 1993, 1994). Single-cell RNA-sequencing analysis of mouse cortex and hippocampus reveals expression ratios of αSyn/βSyn and αSyn/γSyn varying between 0.5 and 2.3, and between 0.002 and 350 in the human cortex, with no detection of γSyn in most cells (Hawrylycz et al., 2012; Lein et al., 2007). While these ratios of mRNA are not guaranteed to reflect protein levels, the differences in mRNA expression are not at odds with the quantified protein levels of each synuclein found throughout the brain (Ahmad et al., 2007; Buchman et al., 1998b; Jakes et al., 1994; Jakowec et al., 2001; Jeannotte et al., 2009; Lavedan, 1998; Lavedan et al., 1998; Maroteaux and Scheller, 1991; Murphy et al., 2000; Ninkina et al., 1998; Ueda et al., 1993, 1994). This vast heterogeneity in levels suggests that relative synuclein ratios may have a functional consequence in modulating synaptic vesicle clustering, SNARE-complex assembly, and neurotransmitter release by regulating the amount of αSyn on synaptic vesicles.

In addition to identifying a physiological role for βSyn and γSyn, our findings may also have implications for the contributions of βSyn and γSyn to disease. βSyn and γSyn have links to several neurodegenerative diseases (Galvin et al., 1999, 2000; Nguyen et al., 2011; Ninkina et al., 2009; Nishioka et al., 2010; Peters et al., 2012; Surgucheva et al., 2002), and missense mutations in βSyn, as well as βSyn or γSyn overexpression, cause neurodegeneration (Fujita et al., 2020; Ninkina et al., 2009; Ohtake et al., 2004; Peters et al., 2012; Psol et al., 2021; Taschenberger et al., 2013). We and others have previously shown that lack of SNARE chaperoning by αSyn or the CSPα chaperone complex causes progressive neuropathology (Burré et al., 2010, 2012, 2015; Greten-Harrison et al., 2010; Sharma et al., 2011, 2012). In addition to a functional loss of αSyn on synaptic vesicles, rendering αSyn less membrane bound through the presence of βSyn and γSyn may increase the aggregation-prone cytosolic pool of αSyn (Figure 7). An alternative hypothesis from some in the field is that formation of membrane-bound αSyn/βSyn or αSyn/γSyn heteromers may shield the aggregation-prone residues in αSyn. These multimers may dissociate from the membrane without immediately converting to their monomeric forms (Dettmer et al., 2017). This shielding of αSyn aggregate-prone regions could be one underlying molecular mechanism for the reported neuroprotection by βSyn (Hashimoto et al., 2001; Windisch et al., 2002), although the neuroprotective effect of βSyn may also be mediated by other pathways, such as regulating cellular survival through Akt or p53 (da Costa et al., 2003; Hashimoto et al., 2004). The relative ratios of the three synucleins may explain the selective vulnerability of certain neuronal populations to dysfunction and degeneration.

Finally, our findings may point to an alternative therapeutic strategy by not only adjusting αSyn levels, but focusing on βSyn and γSyn levels as well. While removal of αSyn can cause functional changes to synapses, particularly in the aged nervous system (Al-Wandi et al., 2010; Benskey et al., 2018; Collier et al.,

2016; Gorbatyuk et al., 2010; Markopoulou et al., 2014; Ninkina et al., 2020; Robertson et al., 2004), approaches targeting βSyn or γSyn to alter aggregation of αSyn may be less detrimental. This could prove to be a particularly attractive strategy, as depleting βSyn and/or γSyn does not result in an αSyn-overexpression phenotype, a hazard to neuronal health (Connor-Robson et al., 2016; Vargas et al., 2014, 2017).

In summary, our data suggest that a correct balance of synucleins is important for normal brain function and that an imbalance of these proteins might affect not only neuron function and plasticity, but also neuronal survival.

Limitations of the study

Our data demonstrate that βSyn and γSyn modulate the synaptic-vesicle-bound pool of αSyn, which mediates αSyn's physiological functions at the synapse. Yet, other studies have not reported a statistically significant enhancement of αSyn function in the absence of βSyn and/or γSyn in comparison with WT neurons. It remains unclear if this is due to the chosen experimental system; e.g., some of these studies involve germline KOs, which may result in other compensatory measures that serve to regulate αSyn levels on vesicles. It is also worth noting that αSyn is thought to have several functions at the synapse, including exocytosis and endocytosis of synaptic vesicles. It is therefore possible that βSyn and γSyn regulate some but not all αSyn activity. As such, previous studies could have closely examined the roles that βSyn and γSyn do not influence. These questions call for further systematic study of the three synuclein family members to better understand their interactions and influence on health and disease.

STAR★METHODS

Detailed methods are provided in the online version of this paper and include the following:

- KEY RESOURCES TABLE
- RESOURCE AVAILABILITY
  - Lead contact
  - Materials availability
  - Data and code availability
- EXPERIMENTAL MODEL AND SUBJECT DETAILS
  - Mice
  - Cell culture and maintenance
- METHOD DETAILS
  - Cell culture and maintenance
  - Immunoprecipitation
  - Subcellular fractionation
  - Quantitative immunoblotting
  - Antibodies
  - Expression vectors
  - Recombinant protein expression
  - Liposome binding assay
  - FRET experiments
  - Circular dichroism spectroscopy
  - Immunocytochemistry
- QUANTIFICATION AND STATISTICAL ANALYSIS

SUPPLEMENTAL INFORMATION

Supplemental information can be found online at https://doi.org/10.1016/j.celrep.2022.110675.

ACKNOWLEDGMENTS

We thank Dr. Thomas C. Südhof for providing antibodies. This work was supported by the Ministry of Science and Higher Education of Russia (agreement 075-15-2021-1346 to V.L.B.), the Alzheimer's Association (NIRG-15-363678 to M.S.), AFAR (M.S.), the Leon Levy Foundation (V.G. and J.B.), and the NIH (R37-AG019391 and R35-GM136686 to D.E., 1R01-AG052505 and 1R01-NS095988 to M.S., R01-NS102181, R01-NS113960, and R01-NS121077 to J.B.).

AUTHOR CONTRIBUTIONS

K.E.C., L.E.K., Y.X.X., A.P., J.A.B., V.G., Y.N., M.S., and J.B. designed the study, performed experiments, and analyzed the data, except for the CD studies, which were designed and performed by T.R. and D.E. V.B. provided the γSyn antibody. K.E.C., L.E.K., and J.B. wrote the manuscript with input from all authors. All authors discussed and commented on the final manuscript.

DECLARATION OF INTERESTS

The authors declare no competing interests.

INCLUSION AND DIVERSITY

We worked to ensure sex balance in the selection of non-human subjects. One or more of the authors of this paper self-identifies as an underrepresented ethnic minority in science.

Received: May 9, 2021
Revised: January 23, 2022
Accepted: March 22, 2022
Published: April 12, 2022

REFERENCES

Abeliovich, A., Schmitz, Y., Farinas, I., Choi-Lundberg, D., Ho, W.H., Castillo, P.E., Shinsky, N., Verdugo, J.M., Armanini, M., Ryan, A., et al. (2000). Mice lacking alpha-synuclein display functional deficits in the nigrostriatal dopamine system. Neuron *25*, 239–252.

Ahmad, M., Attoub, S., Singh, M.N., Martin, F.L., and El-Agnaf, O.M. (2007). Gamma-synuclein and the progression of cancer. FASEB J. *21*, 3419–3430.

Al-Wandi, A., Ninkina, N., Millership, S., Williamson, S.J., Jones, P.A., and Buchman, V.L. (2010). Absence of alpha-synuclein affects dopamine metabolism and synaptic markers in the striatum of aging mice. Neurobiol. Aging *31*, 796–804.

Anderson, J.P., Walker, D.E., Goldstein, J.M., de Laat, R., Banducci, K., Caccavello, R.J., Barbour, R., Huang, J., Kling, K., Lee, M., et al. (2006). Phosphorylation of Ser-129 is the dominant pathological modification of alpha-synuclein in familial and sporadic Lewy body disease. J. Biol. Chem. *281*, 29739–29752.

Arawaka, S., Saito, Y., Murayama, S., and Mori, H. (1998). Lewy body in neurodegeneration with brain iron accumulation type 1 is immunoreactive for alpha-synuclein. Neurology *51*, 887–889.

Atias, M., Tevet, Y., Sun, J., Stavsky, A., Tal, S., Kahn, J., Roy, S., and Gitler, D. (2019). Synapsins regulate alpha-synuclein functions. Proc. Natl. Acad. Sci. U S A *116*, 11116–11118.

Benskey, M.J., Sellnow, R.C., Sandoval, I.M., Sortwell, C.E., Lipton, J.W., and Manfredsson, F.P. (2018). Silencing alpha synuclein in mature nigral neurons results in rapid neuroinflammation and subsequent toxicity. Front. Mol. Neurosci. *11*, 36.

Bertoncini, C.W., Rasia, R.M., Lamberto, G.R., Binolfi, A., Zweckstetter, M., Griesinger, C., and Fernandez, C.O. (2007). Structural characterization of the intrinsically unfolded protein beta-synuclein, a natural negative regulator of alpha-synuclein aggregation. J. Mol. Biol. *372*, 708–722.

Brown, J.W., Buell, A.K., Michaels, T.C., Meisl, G., Carozza, J., Flagmeier, P., Vendruscolo, M., Knowles, T.P., Dobson, C.M., and Galvagnion, C. (2016). beta-Synuclein suppresses both the initiation and amplification steps of alpha-synuclein aggregation via competitive binding to surfaces. Sci. Rep. *6*, 36010.

Buchman, V.L., Adu, J., Pinon, L.G., Ninkina, N.N., and Davies, A.M. (1998a). Persyn, a member of the synuclein family, influences neurofilament network integrity. Nat. Neurosci. *1*, 101–103.

Buchman, V.L., Hunter, H.J., Pinon, L.G., Thompson, J., Privalova, E.M., Ninkina, N.N., and Davies, A.M. (1998b). Persyn, a member of the synuclein family, has a distinct pattern of expression in the developing nervous system. J. Neurosci. *18*, 9335–9341.

Burré, J., Beckhaus, T., Schagger, H., Corvey, C., Hofmann, S., Karas, M., Zimmermann, H., and Volknandt, W. (2006). Analysis of the synaptic vesicle proteome using three gel-based protein separation techniques. Proteomics *6*, 6250–6262.

Burré, J., Sharma, M., and Sudhof, T.C. (2012). Systematic mutagenesis of alpha-synuclein reveals distinct sequence requirements for physiological and pathological activities. J. Neurosci. *32*, 15227–15242.

Burré, J., Sharma, M., and Sudhof, T.C. (2014). alpha-Synuclein assembles into higher-order multimers upon membrane binding to promote SNARE complex formation. Proc. Natl. Acad. Sci. U S A *111*, E4274–E4283.

Burré, J., Sharma, M., and Sudhof, T.C. (2015). Definition of a molecular pathway mediating alpha-synuclein neurotoxicity. J. Neurosci. *35*, 5221–5232.

Burré, J., Sharma, M., Tsetsenis, T., Buchman, V., Etherton, M.R., and Sudhof, T.C. (2010). Alpha-synuclein promotes SNARE-complex assembly in vivo and in vitro. Science *329*, 1663–1667.

Burré, J., Zimmermann, H., and Volknandt, W. (2007). Immunoisolation and subfractionation of synaptic vesicle proteins. Anal. Biochem. *362*, 172–181.

Cabin, D.E., Shimazu, K., Murphy, D., Cole, N.B., Gottschalk, W., McIlwain, K.L., Orrison, B., Chen, A., Ellis, C.E., Paylor, R., et al. (2002). Synaptic vesicle depletion correlates with attenuated synaptic responses to prolonged repetitive stimulation in mice lacking alpha-synuclein. J. Neurosci. *22*, 8797–8807.

Chandra, S., Chen, X., Rizo, J., Jahn, R., and Sudhof, T.C. (2003). A broken alpha -helix in folded alpha -Synuclein. J. Biol. Chem. *278*, 15313–15318.

Chandra, S., Fornai, F., Kwon, H.B., Yazdani, U., Atasoy, D., Liu, X., Hammer, R.E., Battaglia, G., German, D.C., Castillo, P.E., et al. (2004). Double-knockout mice for alpha- and beta-synucleins: effect on synaptic functions. Proc. Natl. Acad. Sci. U S A *101*, 14966–14971.

Chandra, S., Gallardo, G., Fernandez-Chacon, R., Schluter, O.M., and Sudhof, T.C. (2005). Alpha-synuclein cooperates with CSPalpha in preventing neurodegeneration. Cell *123*, 383–396.

Chiba-Falek, O., and Nussbaum, R.L. (2003). Regulation of alpha-synuclein expression: implications for Parkinson's disease. Cold Spring Harb. Symp. Quant. Biol. *68*, 409–415.

Chu, Y., and Kordower, J.H. (2007). Age-associated increases of alpha-synuclein in monkeys and humans are associated with nigrostriatal dopamine depletion: is this the target for Parkinson's disease? Neurobiol. Dis. *25*, 134–149.

Collier, T.J., Redmond, D.E., Jr., Steece-Collier, K., Lipton, J.W., and Manfredsson, F.P. (2016). Is alpha-synuclein loss-of-function a contributor to parkinsonian pathology? Evidence from non-human primates. Front. Neurosci. *10*, 12.

Connor-Robson, N., Peters, O.M., Millership, S., Ninkina, N., and Buchman, V.L. (2016). Combinational losses of synucleins reveal their differential requirements for compensating age-dependent alterations in motor behavior and dopamine metabolism. Neurobiol. Aging *46*, 107–112.

Conway, K.A., Harper, J.D., and Lansbury, P.T. (1998). Accelerated in vitro fibril formation by a mutant alpha-synuclein linked to early-onset Parkinson disease. Nat. Med. *4*, 1318–1320.

Cronin, K.D., Ge, D., Manninger, P., Linnertz, C., Rossoshek, A., Orrison, B.M., Bernard, D.J., El-Agnaf, O.M., Schlossmacher, M.G., Nussbaum, R.L., et al. (2009). Expansion of the Parkinson disease-associated SNCA-Rep1 allele up-regulates human alpha-synuclein in transgenic mouse brain. Hum. Mol. Genet. *18*, 3274–3285.

da Costa, C.A., Masliah, E., and Checler, F. (2003). Beta-synuclein displays an antiapoptotic p53-dependent phenotype and protects neurons from 6-hydroxydopamine-induced caspase 3 activation: cross-talk with alpha-synuclein and implication for Parkinson's disease. J. Biol. Chem. *278*, 37330–37335.

Davidson, W.S., Jonas, A., Clayton, D.F., and George, J.M. (1998). Stabilization of alpha-synuclein secondary structure upon binding to synthetic membranes. J. Biol. Chem. *273*, 9443–9449.

Dettmer, U., Ramalingam, N., von Saucken, V.E., Kim, T.E., Newman, A.J., Terry-Kantor, E., Nuber, S., Ericsson, M., Fanning, S., Bartels, T., et al. (2017). Loss of native alpha-synuclein multimerization by strategically mutating its amphipathic helix causes abnormal vesicle interactions in neuronal cells. Hum. Mol. Genet. *26*, 3466–3481.

Diao, J., Burre, J., Vivona, S., Cipriano, D.J., Sharma, M., Kyoung, M., Sudhof, T.C., and Brunger, A.T. (2013). Native alpha-synuclein induces clustering of synaptic-vesicle mimics via binding to phospholipids and synaptobrevin-2/VAMP2. Elife *2*, e00592.

Ducas, V.C., and Rhoades, E. (2012). Quantifying interactions of beta-synuclein and gamma-synuclein with model membranes. J. Mol. Biol. *423*, 528–539.

Dudek, H., Ghosh, A., and Greenberg, M.E. (2001). Calcium phosphate transfection of DNA into neurons in primary culture. Curr. Protoc. Neurosci. *3*, 3.11.

El-Agnaf, O.M., Jakes, R., Curran, M.D., Middleton, D., Ingenito, R., Bianchi, E., Pessi, A., Neill, D., and Wallace, A. (1998). Aggregates from mutant and wild-type alpha-synuclein proteins and NAC peptide induce apoptotic cell death in human neuroblastoma cells by formation of beta-sheet and amyloid-like filaments. FEBS Lett. *440*, 71–75.

Fujita, M., Ho, G., Takamatsu, Y., Wada, R., Ikeda, K., and Hashimoto, M. (2020). Possible role of amyloidogenic evolvability in dementia with lewy bodies: insights from transgenic mice expressing P123H beta-synuclein. Int. J. Mol. Sci. *21*, 2849.

Fujiwara, H., Hasegawa, M., Dohmae, N., Kawashima, A., Masliah, E., Goldberg, M.S., Shen, J., Takio, K., and Iwatsubo, T. (2002). alpha-Synuclein is phosphorylated in synucleinopathy lesions. Nat. Cell Biol. *4*, 160–164.

Gai, W.P., Power, J.H., Blumbergs, P.C., and Blessing, W.W. (1998). Multiple-system atrophy: a new alpha-synuclein disease? Lancet *352*, 547–548.

Galvin, J.E., Giasson, B., Hurtig, H.I., Lee, V.M., and Trojanowski, J.Q. (2000). Neurodegeneration with brain iron accumulation, type 1 is characterized by alpha-, beta-, and gamma-synuclein neuropathology. Am. J. Pathol. *157*, 361–368.

Galvin, J.E., Uryu, K., Lee, V.M., and Trojanowski, J.Q. (1999). Axon pathology in Parkinson's disease and Lewy body dementia hippocampus contains alpha-, beta-, and gamma-synuclein. Proc. Natl. Acad. Sci. U S A *96*, 13450–13455.

George, J.M. (2002). The synucleins. Genome Biol. *3*, REVIEWS3002.

Gorbatyuk, O.S., Li, S., Nash, K., Gorbatyuk, M., Lewin, A.S., Sullivan, L.F., Mandel, R.J., Chen, W., Meyers, C., Manfredsson, F.P., et al. (2010). In vivo RNAi-mediated alpha-synuclein silencing induces nigrostriatal degeneration. Mol. Ther. *18*, 1450–1457.

Greten-Harrison, B., Polydoro, M., Morimoto-Tomita, M., Diao, L., Williams, A.M., Nie, E.H., Makani, S., Tian, N., Castillo, P.E., Buchman, V.L., et al. (2010). alphabetagamma-Synuclein triple knockout mice reveal age-dependent neuronal dysfunction. Proc. Natl. Acad. Sci. U S A *107*, 19573–19578.

Hashimoto, M., Bar-On, P., Ho, G., Takenouchi, T., Rockenstein, E., Crews, L., and Masliah, E. (2004). Beta-synuclein regulates Akt activity in neuronal cells. A possible mechanism for neuroprotection in Parkinson's disease. J. Biol. Chem. *279*, 23622–23629.

Hashimoto, M., Rockenstein, E., Mante, M., Mallory, M., and Masliah, E. (2001). beta-Synuclein inhibits alpha-synuclein aggregation: a possible role as an anti-parkinsonian factor. Neuron *32*, 213–223.

Hawrylycz, M.J., Lein, E.S., Guillozet-Bongaarts, A.L., Shen, E.H., Ng, L., Miller, J.A., van de Lagemaat, L.N., Smith, K.A., Ebbert, A., Riley, Z.L., et al. (2012). An anatomically comprehensive atlas of the adult human brain transcriptome. Nature *489*, 391–399.

Ibanez, P., Bonnet, A.M., Debarges, B., Lohmann, E., Tison, F., Pollak, P., Agid, Y., Durr, A., and Brice, A. (2004). Causal relation between alpha-synuclein gene duplication and familial Parkinson's disease. Lancet *364*, 1169–1171.

Iwai, A., Masliah, E., Yoshimoto, M., Ge, N., Flanagan, L., de Silva, H.A., Kittel, A., and Saitoh, T. (1995). The precursor protein of non-A beta component of Alzheimer's disease amyloid is a presynaptic protein of the central nervous system. Neuron *14*, 467–475.

Jain, M.K., Singh, P., Roy, S., and Bhat, R. (2018). Comparative analysis of the conformation, aggregation, interaction, and fibril morphologies of human alpha-, beta-, and gamma-synuclein proteins. Biochemistry *57*, 3830–3848.

Jakes, R., Spillantini, M.G., and Goedert, M. (1994). Identification of two distinct synucleins from human brain. FEBS Lett. *345*, 27–32.

Jakowec, M.W., Donaldson, D.M., Barba, J., and Petzinger, G.M. (2001). Postnatal expression of alpha-synuclein protein in the rodent substantia nigra and striatum. Dev. Neurosci. *23*, 91–99.

Janowska, M.K., Wu, K.P., and Baum, J. (2015). Unveiling transient protein-protein interactions that modulate inhibition of alpha-synuclein aggregation by beta-synuclein, a pre-synaptic protein that co-localizes with alpha-synuclein. Sci. Rep. *5*, 15164.

Jeannotte, A.M., McCarthy, J.G., Redei, E.E., and Sidhu, A. (2009). Desipramine modulation of alpha-, gamma-synuclein, and the norepinephrine transporter in an animal model of depression. Neuropsychopharmacology *34*, 987–998.

Ji, H., Liu, Y.E., Jia, T., Wang, M., Liu, J., Xiao, G., Joseph, B.K., Rosen, C., and Shi, Y.E. (1997). Identification of a breast cancer-specific gene, BCSG1, by direct differential cDNA sequencing. Cancer Res. *57*, 759–764.

Jiang, Y., Liu, Y.E., Goldberg, I.D., and Shi, Y.E. (2004). Gamma synuclein, a novel heat-shock protein-associated chaperone, stimulates ligand-dependent estrogen receptor alpha signaling and mammary tumorigenesis. Cancer Res. *64*, 4539–4546.

Kahle, P.J., Neumann, M., Ozmen, L., Muller, V., Jacobsen, H., Schindzielorz, A., Okochi, M., Leimer, U., van Der Putten, H., Probst, A., et al. (2000). Subcellular localization of wild-type and Parkinson's disease-associated mutant alpha -synuclein in human and transgenic mouse brain. J. Neurosci. *20*, 6365–6373.

Kuhn, M., Haebig, K., Bonin, M., Ninkina, N., Buchman, V.L., Poths, S., and Riess, O. (2007). Whole genome expression analyses of single- and double-knock-out mice implicate partially overlapping functions of alpha- and gamma-synuclein. Neurogenetics *8*, 71–81.

Lautenschlager, J., Stephens, A.D., Fusco, G., Strohl, F., Curry, N., Zacharopoulou, M., Michel, C.H., Laine, R., Nespovitaya, N., Fantham, M., et al. (2018). C-terminal calcium binding of alpha-synuclein modulates synaptic vesicle interaction. Nat. Commun. *9*, 712.

Lavedan, C. (1998). The synuclein family. Genome Res. *8*, 871–880.

Lavedan, C., Leroy, E., Dehejia, A., Buchholtz, S., Dutra, A., Nussbaum, R.L., and Polymeropoulos, M.H. (1998). Identification, localization and characterization of the human gamma-synuclein gene. Hum. Genet. *103*, 106–112.

Lein, E.S., Hawrylycz, M.J., Ao, N., Ayres, M., Bensinger, A., Bernard, A., Boe, A.F., Boguski, M.S., Brockway, K.S., Byrnes, E.J., et al. (2007). Genome-wide atlas of gene expression in the adult mouse brain. Nature *445*, 168–176.

Linnertz, C., Saucier, L., Ge, D., Cronin, K.D., Burke, J.R., Browndyke, J.N., Hulette, C.M., Welsh-Bohmer, K.A., and Chiba-Falek, O. (2009). Genetic regulation of alpha-synuclein mRNA expression in various human brain tissues. PLoS One *4*, e7480.

Maraganore, D.M., de Andrade, M., Elbaz, A., Farrer, M.J., Ioannidis, J.P., Kruger, R., Rocca, W.A., Schneider, N.K., Lesnick, T.G., Lincoln, S.J., et al. (2006). Collaborative analysis of alpha-synuclein gene promoter variability and Parkinson disease. JAMA *296*, 661–670.

Markopoulou, K., Biernacka, J.M., Armasu, S.M., Anderson, K.J., Ahlskog, J.E., Chase, B.A., Chung, S.J., Cunningham, J.M., Farrer, M., Frigerio, R., et al. (2014). Does alpha-synuclein have a dual and opposing effect in preclinical vs. clinical Parkinson's disease? Parkinsonism Relat. Disord. *20*, 584–589.

Maroteaux, L., Campanelli, J.T., and Scheller, R.H. (1988). Synuclein: a neuron-specific protein localized to the nucleus and presynaptic nerve terminal. J. Neurosci. *8*, 2804–2815.

Maroteaux, L., and Scheller, R.H. (1991). The rat brain synucleins; family of proteins transiently associated with neuronal membrane. Brain Res. Mol. Brain Res. *11*, 335–343.

Middleton, E.R., and Rhoades, E. (2010). Effects of curvature and composition on alpha-synuclein binding to lipid vesicles. Biophys. J. *99*, 2279–2288.

Morciano, M., Burre, J., Corvey, C., Karas, M., Zimmermann, H., and Volknandt, W. (2005). Immunoisolation of two synaptic vesicle pools from synaptosomes: a proteomics analysis. J. Neurochem. *95*, 1732–1745.

Murphy, D.D., Rueter, S.M., Trojanowski, J.Q., and Lee, V.M. (2000). Synucleins are developmentally expressed, and alpha-synuclein regulates the size of the presynaptic vesicular pool in primary hippocampal neurons. J. Neurosci. *20*, 3214–3220.

Nakajo, S., Tsukada, K., Omata, K., Nakamura, Y., and Nakaya, K. (1993). A new brain-specific 14-kDa protein is a phosphoprotein. Its complete amino acid sequence and evidence for phosphorylation. Eur. J. Biochem. *217*, 1057–1063.

Nguyen, J.V., Soto, I., Kim, K.Y., Bushong, E.A., Oglesby, E., Valiente-Soriano, F.J., Yang, Z., Davis, C.H., Bedont, J.L., Son, J.L., et al. (2011). Myelination transition zone astrocytes are constitutively phagocytic and have synuclein dependent reactivity in glaucoma. Proc. Natl. Acad. Sci. U S A *108*, 1176–1181.

Ninkina, N., Millership, S.J., Peters, O.M., Connor-Robson, N., Chaprov, K., Kopylov, A.T., Montoya, A., Kramer, H., Withers, D.J., and Buchman, V.L. (2021). beta-synuclein potentiates synaptic vesicle dopamine uptake and rescues dopaminergic neurons from MPTP-induced death in the absence of other synucleins. J. Biol. Chem. *297*, 101375.

Ninkina, N., Papachroni, K., Robertson, D.C., Schmidt, O., Delaney, L., O'Neill, F., Court, F., Rosenthal, A., Fleetwood-Walker, S.M., Davies, A.M., et al. (2003). Neurons expressing the highest levels of gamma-synuclein are unaffected by targeted inactivation of the gene. Mol. Cell Biol. *23*, 8233–8245.

Ninkina, N., Peters, O., Millership, S., Salem, H., van der Putten, H., and Buchman, V.L. (2009). Gamma-synucleinopathy: neurodegeneration associated with overexpression of the mouse protein. Hum. Mol. Genet. *18*, 1779–1794.

Ninkina, N., Peters, O.M., Connor-Robson, N., Lytkina, O., Sharfeddin, E., and Buchman, V.L. (2012). Contrasting effects of alpha-synuclein and gamma-synuclein on the phenotype of cysteine string protein alpha (CSPalpha) null mutant mice suggest distinct function of these proteins in neuronal synapses. J. Biol. Chem. *287*, 44471–44477.

Ninkina, N., Tarasova, T.V., Chaprov, K.D., Roman, A.Y., Kukharsky, M.S., Kolik, L.G., Ovchinnikov, R., Ustyugov, A.A., Durnev, A.D., and Buchman, V.L. (2020). Alterations in the nigrostriatal system following conditional inactivation of alpha-synuclein in neurons of adult and aging mice. Neurobiol. Aging *91*, 76–87.

Ninkina, N.N., Alimova-Kost, M.V., Paterson, J.W., Delaney, L., Cohen, B.B., Imreh, S., Gnuchev, N.V., Davies, A.M., and Buchman, V.L. (1998). Organization, expression and polymorphism of the human persyn gene. Hum. Mol. Genet. *7*, 1417–1424.

Nishioka, K., Wider, C., Vilarino-Guell, C., Soto-Ortolaza, A.I., Lincoln, S.J., Kachergus, J.M., Jasinska-Myga, B., Ross, O.A., Rajput, A., Robinson, C.A., et al. (2010). Association of alpha-, beta-, and gamma-Synuclein with diffuse lewy body disease. Arch. Neurol. *67*, 970–975.

Ohtake, H., Limprasert, P., Fan, Y., Onodera, O., Kakita, A., Takahashi, H., Bonner, L.T., Tsuang, D.W., Murray, I.V., Lee, V.M., et al. (2004). Beta-synuclein gene alterations in dementia with Lewy bodies. Neurology *63*, 805–811.

Papachroni, K., Ninkina, N., Wanless, J., Kalofoutis, A.T., Gnuchev, N.V., and Buchman, V.L. (2005). Peripheral sensory neurons survive in the absence of alpha- and gamma-synucleins. J. Mol. Neurosci. *25*, 157–164.

Park, J.Y., and Lansbury, P.T., Jr. (2003). Beta-synuclein inhibits formation of alpha-synuclein protofibrils: a possible therapeutic strategy against Parkinson's disease. Biochemistry *42*, 3696–3700.

Peters, O.M., Millership, S., Shelkovnikova, T.A., Soto, I., Keeling, L., Hann, A., Marsh-Armstrong, N., Buchman, V.L., and Ninkina, N. (2012). Selective pattern of motor system damage in gamma-synuclein transgenic mice mirrors the respective pathology in amyotrophic lateral sclerosis. Neurobiol. Dis. *48*, 124–131.

Psol, M., Darvas, S.G., Leite, K., Mahajani, S.U., Bahr, M., and Kugler, S. (2021). Dementia with Lewy bodies-associated beta-synuclein mutations V70M and P123H cause mutation-specific neuropathological lesions. Hum. Mol. Genet. *30*, 247–264.

Rao, J.N., Kim, Y.E., Park, L.S., and Ulmer, T.S. (2009). Effect of pseudorepeat rearrangement on alpha-synuclein misfolding, vesicle binding, and micelle binding. J. Mol. Biol. *390*, 516–529.

Rivers, R.C., Kumita, J.R., Tartaglia, G.G., Dedmon, M.M., Pawar, A., Vendruscolo, M., Dobson, C.M., and Christodoulou, J. (2008). Molecular determinants of the aggregation behavior of alpha- and beta-synuclein. Protein Sci. *17*, 887–898.

Robertson, D.C., Schmidt, O., Ninkina, N., Jones, P.A., Sharkey, J., and Buchman, V.L. (2004). Developmental loss and resistance to MPTP toxicity of dopaminergic neurones in substantia nigra pars compacta of gamma-synuclein, alpha-synuclein and double alpha/gamma-synuclein null mutant mice. J. Neurochem. *89*, 1126–1136.

Rocha, S., Kumar, R., Horvath, I., and Wittung-Stafshede, P. (2019). Synaptic vesicle mimics affect the aggregation of wild-type and A53T alpha-synuclein variants differently albeit similar membrane affinity. Protein Eng. Des. Sel *32*, 59–66.

Rochet, J.C., Conway, K.A., and Lansbury, P.T., Jr. (2000). Inhibition of fibrillization and accumulation of prefibrillar oligomers in mixtures of human and mouse alpha-synuclein. Biochemistry *39*, 10619–10626.

Sanjeev, A., Sahu, R.K., and Mattaparthi, V.S.K. (2017). Potential of mean force and molecular dynamics study on the transient interactions between alpha and beta synuclein that drive inhibition of alpha-synuclein aggregation. J. Biomol. Struct. Dyn. *35*, 3342–3353.

Schluter, O.M., Fornai, F., Alessandri, M.G., Takamori, S., Geppert, M., Jahn, R., and Sudhof, T.C. (2003). Role of alpha-synuclein in 1-methyl-4-phenyl-1,2,3,6-tetrahydropyridine-induced parkinsonism in mice. Neuroscience *118*, 985–1002.

Scott, D., and Roy, S. (2012). alpha-Synuclein inhibits intersynaptic vesicle mobility and maintains recycling-pool homeostasis. J. Neurosci. *32*, 10129–10135.

Senior, S.L., Ninkina, N., Deacon, R., Bannerman, D., Buchman, V.L., Cragg, S.J., and Wade-Martins, R. (2008). Increased striatal dopamine release and hyperdopaminergic-like behaviour in mice lacking both alpha-synuclein and gamma-synuclein. Eur. J. Neurosci. *27*, 947–957.

Sharma, K., Mehra, S., Sawner, A.S., Markam, P.S., Panigrahi, R., Navalkar, A., Chatterjee, D., Kumar, R., Kadu, P., Patel, K., et al. (2020). Effect of disease-associated P123H and V70M mutations on beta-synuclein fibrillation. ACS Chem. Neurosci. *11*, 2836–2848.

Sharma, M., Burre, J., Bronk, P., Zhang, Y., Xu, W., and Sudhof, T.C. (2012). CSPalpha knockout causes neurodegeneration by impairing SNAP-25 function. EMBO J. *31*, 829–841.

Sharma, M., Burre, J., and Sudhof, T.C. (2011). CSPalpha promotes SNARE-complex assembly by chaperoning SNAP-25 during synaptic activity. Nat. Cell Biol. *13*, 30–39.

Singleton, A.B., Farrer, M., Johnson, J., Singleton, A., Hague, S., Kachergus, J., Hulihan, M., Peuralinna, T., Dutra, A., Nussbaum, R., et al. (2003). alpha-Synuclein locus triplication causes Parkinson's disease. Science *302*, 841.

Spillantini, M.G., Schmidt, M.L., Lee, V.M., Trojanowski, J.Q., Jakes, R., and Goedert, M. (1997). Alpha-synuclein in lewy bodies. Nature *388*, 839–840.

Sun, J., Wang, L., Bao, H., Premi, S., Das, U., Chapman, E.R., and Roy, S. (2019). Functional cooperation of alpha-synuclein and VAMP2 in synaptic vesicle recycling. Proc. Natl. Acad. Sci. U S A *116*, 11113–11115.

Sung, Y.H., and Eliezer, D. (2006). Secondary structure and dynamics of micelle bound beta- and gamma-synuclein. Protein Sci. *15*, 1162–1174.

Surgucheva, I., McMahan, B., Ahmed, F., Tomarev, S., Wax, M.B., and Surguchov, A. (2002). Synucleins in glaucoma: implication of gamma-synuclein in glaucomatous alterations in the optic nerve. J. Neurosci. Res. *68*, 97–106.

Surgucheva, I., Ninkina, N., Buchman, V.L., Grasing, K., and Surguchov, A. (2005). Protein aggregation in retinal cells and approaches to cell protection. Cell Mol. Neurobiol. *25*, 1051–1066.

Takamori, S., Holt, M., Stenius, K., Lemke, E.A., Gronborg, M., Riedel, D., Urlaub, H., Schenck, S., Brugger, B., Ringler, P., et al. (2006). Molecular anatomy of a trafficking organelle. Cell *127*, 831–846.

Tao-Cheng, J.H. (2006). Activity-related redistribution of presynaptic proteins at the active zone. Neuroscience *141*, 1217–1224.

Taoufiq, Z., Ninov, M., Villar-Briones, A., Wang, H.Y., Sasaki, T., Roy, M.C., Beauchain, F., Mori, Y., Yoshida, T., Takamori, S., et al. (2020). Hidden proteome of synaptic vesicles in the mammalian brain. Proc. Natl. Acad. Sci. U S A *117*, 33586–33596.

Taschenberger, G., Toloe, J., Tereshchenko, J., Akerboom, J., Wales, P., Benz, R., Becker, S., Outeiro, T.F., Looger, L.L., Bahr, M., et al. (2013). beta-synuclein aggregates and induces neurodegeneration in dopaminergic neurons. Ann. Neurol. *74*, 109–118.

Tsigelny, I.F., Bar-On, P., Sharikov, Y., Crews, L., Hashimoto, M., Miller, M.A., Keller, S.H., Platoshyn, O., Yuan, J.X., and Masliah, E. (2007). Dynamics of alpha-synuclein aggregation and inhibition of pore-like oligomer development by beta-synuclein. FEBS J. *274*, 1862–1877.

Ueda, K., Fukushima, H., Masliah, E., Xia, Y., Iwai, A., Yoshimoto, M., Otero, D.A., Kondo, J., Ihara, Y., and Saitoh, T. (1993). Molecular cloning of cDNA encoding an unrecognized component of amyloid in Alzheimer disease. Proc. Natl. Acad. Sci. U S A *90*, 11282–11286.

Ueda, K., Saitoh, T., and Mori, H. (1994). Tissue-dependent alternative splicing of mRNA for NACP, the precursor of non-A beta component of Alzheimer's disease amyloid. Biochem. Biophys. Res. Commun. *205*, 1366–1372.

Uversky, V.N., Li, J., Souillac, P., Millett, I.S., Doniach, S., Jakes, R., Goedert, M., and Fink, A.L. (2002). Biophysical properties of the synucleins and their propensities to fibrillate: inhibition of alpha-synuclein assembly by beta- and gamma-synucleins. J. Biol. Chem. *277*, 11970–11978.

Van de Vondel, E., Baatsen, P., Van Elzen, R., Lambeir, A.M., Keiderling, T.A., Herrebout, W.A., and Johannessen, C. (2018). Vibrational circular dichroism sheds new light on the competitive effects of crowding and beta-synuclein on the fibrillation process of alpha-synuclein. Biochemistry *57*, 5989–5995.

Vargas, K.J., Makani, S., Davis, T., Westphal, C.H., Castillo, P.E., and Chandra, S.S. (2014). Synucleins regulate the kinetics of synaptic vesicle endocytosis. J. Neurosci. *34*, 9364–9376.

Vargas, K.J., Schrod, N., Davis, T., Fernandez-Busnadiego, R., Taguchi, Y.V., Laugks, U., Lucic, V., and Chandra, S.S. (2017). Synucleins have multiple effects on presynaptic architecture. Cell Rep. *18*, 161–173.

Wakabayashi, K., Matsumoto, K., Takayama, K., Yoshimoto, M., and Takahashi, H. (1997). NACP, a presynaptic protein, immunoreactivity in Lewy bodies in Parkinson's disease. Neurosci. Lett. *239*, 45–48.

Westphal, C.H., and Chandra, S.S. (2013). Monomeric synucleins generate membrane curvature. J. Biol. Chem. *288*, 1829–1840.

Windisch, M., Hutter-Paier, B., Rockenstein, E., Hashimoto, M., Mallory, M., and Masliah, E. (2002). Development of a new treatment for Alzheimer's disease and Parkinson's disease using anti-aggregatory beta-synuclein-derived peptides. J. Mol. Neurosci. *19*, 63–69.

Yavich, L., Tanila, H., Vepsalainen, S., and Jakala, P. (2004). Role of alpha-synuclein in presynaptic dopamine recruitment. J. Neurosci. *24*, 11165–11170.

Zhang, H., Kouadio, A., Cartledge, D., and Godwin, A.K. (2011). Role of gamma-synuclein in microtubule regulation. Exp. Cell Res. *317*, 1330–1339.

STAR★METHODS

KEY RESOURCES TABLE

REAGENT or RESOURCE	SOURCE	IDENTIFIER
Antibodies		
CSPα	Dr. Thomas C. Südhof	R807
GAPDH	Santa Cruz	Cat# sc-365062, RRID:AB_10847862
MAP2	Millipore	Cat# AB5622, RRID:AB_91939
MAP2	Sigma	Cat# M1406, RRID:AB_477171
Myc	DSHB; deposited by Bishop, J.M.	Cat# 9E 10, RRID:AB_2266850
Myc	Sigma	Cat# C3956, RRID:AB_439680
VDAC1	Neuromab	Cat# N152B/23, RRID:AB_2877354
Na,K-ATPase	DSHB; deposited by Fambrough, D.M.	Cat# a5, RRID:AB_2166869
NF-165	DSHB; deposited by Jessell, T.M./Dodd, J.	Cat# 2H3, RRID:AB_531793
SNAP-25	Covance	Cat# SMI-81, RRID:AB_2315336
Synapsin	Dr. Thomas C. Südhof	E028
Synaptobrevin-2	Synaptic Systems	Cat# 104 211, RRID:AB_887811
Synaptophysin	Synaptic Systems	Cat# 101 011, RRID:AB_887824
αSyn	BD Biosystems	Cat# 610787, RRID:AB_398108
αSyn	Abcam	Cat# ab1903, RRID:AB_302665
βSyn	Santa Cruz	Cat# sc-136452, RRID:AB_10609953
γSyn	Dr. Vladimir Buchman	SK23
pS129 αSyn	FUJIFILM Wako	Cat# 015-25191, RRID:AB_2537218
SV2	Dr. Thomas C. Südhof	P915
SV2	DSHB; deposited by Buckley, K.M.	Cat# SV2, RRID:AB_2315387
α-Tubulin	DSHB; deposited by Frankel, J./Nelsen, E.M.	Cat# 12G10 anti-alpha-tubulin, RRID:AB_1157911
Tuj1	Santa Cruz	Cat# sc-80005, RRID:AB_2210816
Tyrosine hydroxylase	Millipore	Cat# MAB318, RRID:AB_2201528
Bacterial and virus strains		
BL21(DE3)	Thermo Fisher	EC0114
DH5α	Thermo Fisher	18265017
Biological samples		
Egg L-α-phosphatidylcholine (PC)	Avanti Polar Lipids	840051C
Brain L-α-phosphatidylethanolamine (PE)	Avanti Polar Lipids	840022C
Brain L-α-phosphatidylserine (PS)	Avanti Polar Lipids	840032C
Liver L-α-phosphatidylinositol (PI)	Avanti Polar Lipids	840042C
Brain sphingomyelin (SM)	Avanti Polar Lipids	860062C
Cholesterol	Avanti Polar Lipids	700000P
Chemicals, peptides, and recombinant proteins		
Alexa 488 C5 maleimide	Thermo Fisher	A10254
Alexa 546 C5 maleimide	Thermo Fisher	A10258
Pierce Glutathione Superflow Agarose Affinity Chromatography Media	Thermo Fisher	25238
Protein A - Sepharose 4B	Thermo Fisher	101041
Dynabeads Protein G	Thermo Fisher	10019D
Experimental models: Cell lines		
HEK293T	ATCC	CRL-3216
Experimental models: Organisms/strains		
αβγSyn knockout mice	Burré et al., 2010	N/A

(*Continued on next page*)

Continued

REAGENT or RESOURCE	SOURCE	IDENTIFIER
αSyn knockout mice	This manuscript	N/A
βSyn knockout mice	This manuscript	N/A
γSyn knockout mice	This manuscript	N/A
Wild-type	Jackson Laboratories	C57BL/6J
Recombinant DNA		
pGEX-KG myc αSyn	Burré et al., 2010	N/A
pGEX-KG myc αSyn 1-95	Burré et al., 2010	N/A
pGEX-KG myc αSyn L8C	This manuscript	N/A
pGEX-KG myc αSyn K96C	This manuscript	N/A
pGEX-KG myc βSyn	This manuscript	N/A
pGEX-KG myc βSyn 1-85	This manuscript	N/A
pGEX-KG myc βSyn L8C	This manuscript	N/A
pGEX-KG myc βSyn K85C	This manuscript	N/A
pGEX-KG myc γSyn	This manuscript	N/A
pGEX-KG myc γSyn 1-96	This manuscript	N/A
pGEX-KG myc γSyn F8C	This manuscript	N/A
pGEX-KG myc γSyn K96C	This manuscript	N/A
pCMV5 myc αSyn	Burré et al., 2010	N/A
pCMV5 myc βSyn	This manuscript	N/A
pCMV5 myc γSyn	This manuscript	N/A
FUW myc αSyn	Burré et al., 2010	N/A
FUW myc βSyn	This manuscript	N/A
FUW myc γSyn	This manuscript	N/A
pMD2-G-VSVg	Gift from Didier Trono; Addgene	12259
pRSV-Rev	Gift from Didier Trono; Addgene	12253
pMDLg/pRRE	Gift from Didier Trono; Addgene	12251
FSW Td-Tomato	This study	N/A
Software and algorithms		
Photoshop	Adobe	https://www.adobe.com/products/photoshop.html
ImageJ	NIH	https://imagej.nih.gov/ij/
Image Studio	LI-COR Biosciences	https://www.licor.com/bio/image-studio/
Prism 8 Software	GraphPad	https://www.graphpad.com/scientific-software/prism/
Illustrator	Adobe	https://www.adobe.com/products/illustrator.html

RESOURCE AVAILABILITY

Lead contact

Further information and requests for resources and reagents should be directed to and will be fulfilled by the Lead Contact, Jacqueline Burré (jab2058@med.cornell.edu).

Materials availability

All unique/stable reagents including plasmids for expression of β- and γ-synuclein and synuclein knockout mouse lines that were generated in this study are available from the Lead contact with a completed Materials Transfer Agreement.

Data and code availability

- All data reported in this paper will be shared by the Lead contact upon request.
- This paper does not report original code.
- Any additional information required to reanalyze the data reported in this paper is available from the Lead contact upon request.

EXPERIMENTAL MODEL AND SUBJECT DETAILS

Mice

Wild-type and synuclein null mice were maintained on a C57BL/6 background (Jackson labs). Synuclein triple knockout mice were maintained as described previously (Burré et al., 2010). αSyn, βSyn, and γSyn single knockout mouse lines were generated by crossing the synuclein triple knockout mice to wild type C57BL/6 mice, and then back crossing the triple-hemizygous progeny to wild-type progeny for 5 generations before separating each of the synuclein knockout alleles. Mice of either sex were used for neuronal culture, and no inclusion criteria were used. Mice were housed with a 12-h light/dark cycle in a temperature-controlled room with free access to water and food. All animal procedures were performed according to NIH guidelines and approved by the Committee on Animal Care at Weill Cornell Medicine.

Cell culture and maintenance

HEK293T cells (ATCC) were maintained in DMEM with 1% penicillin and streptomycin and 10% bovine serum at 37°C and 5% CO_2. Cells were not authenticated.

METHOD DETAILS

Cell culture and maintenance

For production of lentiviral vectors, HEK293T cells were transfected with equimolar amounts of lentiviral vector FUW containing myc-tagged or untagged αSyn, βSyn, or γSyn, pMD2-G-VSVg (Addgene # 12259, a gift from Didier Trono), pMDLg/pRRE (Addgene # 12253, a gift from Didier Trono), and pRSV-Rev (Addgene # 12251, a gift from Didier Trono) using calcium phosphate produced in house. 1 h prior to transfection, 25 μM chloroquine in fresh media was added. DNA was incubated for 1 min at room temperature in 100 mM $CaCl_2$ and 1× HBS (25 mM HEPES pH 7.05, 140 mM NaCl, and 0.75 mM Na_2HPO_4) and the transfection mix was then slowly added to the cells. Medium was replaced with fresh medium after 6 h. Medium containing the viral particles was collected 48 h later and centrifuged for 10 min at 500 g_{av} to remove cellular debris. Viral particles were subsequently concentrated tenfold by centrifugation. Mouse cortical neurons or mouse midbrain neurons were cultured from newborn mice of either sex. Cortices were dissected in ice-cold HBSS, dissociated and triturated with a siliconized pipette, and plated onto 6 mm poly l-lysine-coated coverslips (for immunofluorescence) or on 24-well plastic dishes. Plating media (MEM supplemented with 5 g/L glucose, 0.2 g/L $NaHCO_3$, 0.1 g/L transferrin, 0.25 g/L insulin, 0.3 g/l L-glutamine, and 10% fetal bovine serum) was replaced with growth media (MEM containing 5 g/L glucose, 0.2 g/L $NaHCO_3$, 0.1 g/L transferrin, 0.3 g/l L-glutamine, 5% fetal bovine serum, 2% B-27 supplement, and 2 μM cytosine arabinoside) 2 days after plating. At 6 days *in vitro* (DIV), neurons were transduced with recombinant lentiviruses expressing synucleins or transfected with pCMV5 myc-αSyn. Calcium phosphate transfections were performed as previously described (Dudek et al., 2001). Transduced neurons were harvested or used for experiments as indicated at 27 DIV, transfected neurons at 14 DIV.

Immunoprecipitation

Transfected HEK293T cells were solubilized in PBS, pH 7.4, containing 0.15% Triton X-100 and protease inhibitors (VWR). Following centrifugation at 16,000 g_{av} for 20 min at 4°C, the clarified lysate was used for immunoblotting (after addition of 2× SDS sample buffer containing 100 mM DTT) or subjected to immunoprecipitation. Immunoprecipitation was performed with the indicated primary antibodies and 50 μL of a 50% slurry of protein-A Sepharose beads (Thermo Fisher) for 2 h at 4°C. Control immunoprecipitations were performed with preimmune sera. Following five washes with 1 mL of the extraction buffer, bound proteins were eluted with 2× SDS sample buffer containing 100 mM DTT and boiled for 20 min at 100°C. Co-precipitated proteins were separated by SDS-PAGE, with 5% of the input in the indicated lane. Immunoisolation of synaptic vesicles was done as previously described (Burré et al., 2006, 2007). Immunoprecipitated vesicles (50 μg) were then incubated on magnetic beads (Thermo Fisher) with 350 nM αSyn, 350 nM βSyn, 350 nM γSyn, or 350 nM αSyn plus either 350 nM or 1400 nM βSyn, or 350 nM αSyn plus either 350 nM or 1400 nM γSyn. Beads were washed three times with PBS and bound proteins were eluted with 2× SDS sample buffer containing 100 mM DTT. Precipitated synucleins were separated by SDS-PAGE, with 5% of synaptic vesicles and 50% of synucleins as input.

Subcellular fractionation

For cytosol/membrane fractionations, entire mouse brains were homogenized in PBS containing protease inhibitors. The homogenates were centrifuged for 1 h at 300,000 g_{av}. The supernatant was collected and an equal volume of PBS was added to the pellet. Same volumes were analyzed via SDS-PAGE. Synaptosomes were isolated as previously described (Burré et al., 2006). Briefly, entire mouse brains were homogenized in preparation buffer (5 mM Tris-HCl, 320 mM sucrose, pH 7.4), supplemented with protease inhibitors. The homogenate was centrifuged for 10 min at 1,000 g_{av}. The supernatant was collected and the pellet was resuspended in preparation buffer and recentrifuged. Both supernatants were pooled and the final pellet was discarded. Discontinuous Percoll gradients were prepared by layering 7.5 mL supernatant onto three layers of 7.5 mL Percoll solution (3%, 10%, and 23% v/v in 320 mM sucrose, 5 mM Tris-HCl, pH 7.4). After centrifugation for 7 min at 31,400 g_{av}, fractions containing synaptosomes were

collected, diluted in four volumes of preparation buffer and centrifuged for 35 min at 20,000 g_{av}. Synaptic vesicles were isolated from osmotically lysed synaptosomes as previously described (Burré et al., 2006). Briefly, synaptosomal pellets were resuspended in lysis buffer (5 mM Tris-HCl, pH 7.4). The suspension was centrifuged for 1 h at 188,000 g_{av}, and the pellet was resuspended in 4 mL of sucrose gradient buffer (200 mM sucrose, 0.1 mM $MgCl_2$, 0.5 mM EGTA, 10 mM HEPES-NaOH, pH 7.4) and homogenized. The resulting suspension was layered onto a continuous sucrose gradient ranging from 0.3 M to 1.2 M sucrose (sucrose in 10 mM HEPES-NaOH, 0.5 mM EGTA, pH 7.4) and centrifuged for 2 h at 85,000 g_{av}. Thirty-six 1 mL fractions were collected from top to the bottom of the gradient.

Quantitative immunoblotting

Protein samples were separated by SDS-PAGE and either stained using Coomassie Brilliant Blue, or transferred onto nitrocellulose membranes. Blots were blocked in Tris-buffered saline (TBS) containing 0.1% Tween 20 (TBS-T) containing 5% fat-free milk for 30 min at room temperature. The blocked membrane was incubated overnight in PBS containing 1% BSA and 0.2% NaN_3 and the primary antibody. The blots were then washed twice in TBS-T containing 5% fat-free milk, then incubated for 1 h in the same buffer containing secondary antibody at room temperature. Blots were then washed 3 times in TBS-T, twice in water, and then dried in the dark. Blots were imaged using an LI-COR Odyssey CLx, and images were analyzed using ImageStudioLite (LI-COR).

Antibodies

CSPα (R807, gift from Dr. Thomas C. Südhof), GAPDH (G-9, Santa Cruz), MAP2 (AB5622, Millipore; M1406, Sigma), myc (9E10, deposited to the DSHB by Bishop, J.M.; C3956, Sigma), VDAC1 (N152B/23, Neuromab), Na,K-ATPase (a5, deposited to the DSHB by Fambrough, D.M.), NF-165 (2H3, deposited to the DSHB by Jessell, T.M./Dodd, J.), SNAP-25 (SMI81, Sternberger Monoclonals), synapsin (E028, gift from Dr. Thomas C. Südhof), synaptobrevin-2 (69.1, Synaptic Systems), synaptophysin (clone 7.2, Synaptic Systems), αSyn (clone 42, BD Biosystems; clone 4D6, Abcam), βSyn (sc-136452, Santa Cruz), γSyn (SK23 (Ninkina et al., 2003)), pS129 αSyn (pSyn #64, FUJIFILM Wako), SV2 (P915, gift from Dr. Thomas C. Südhof; SV2, deposited to the DSHB by Buckley, K.M.), α-tubulin (12G10, DSHB), Tuj1 (2G10, Santa Cruz), and tyrosine hydroxylase (MAB318, Millipore).

Expression vectors

Full-length human αSyn, βSyn, or γSyn cDNA was inserted into modified pGEX-KG vectors (GE Healthcare) containing an N-terminal TEV protease recognition site, or into lentiviral vector FUW, without or with an N-terminal myc-tag and a four amino acid linker, resulting in the following N-terminal sequence (EQKLISEEDL-GSGS). Lentiviral and pCMV5 myc-αSyn were subcloned from pGEX-KG myc-αSyn. Mutant αSyn, βSyn, or γSyn constructs were generated by site-specific mutagenesis, according to the protocol of the manufacturer (Stratagene). For analysis of subcellular localization, TdTomato was inserted into an FSW lentiviral vector, enabling expression of TdTomato driven by the synapsin promoter. Plasmids were amplified by expression in DH5a (Thermo Fisher).

Recombinant protein expression

All proteins were expressed as GST fusion proteins in bacteria (BL21 strain, Thermo Fisher), essentially as described (Burré et al., 2010). Bacteria were grown to OD 0.6 (measured at 600 nm), and protein expression was induced with 0.05 mM isopropyl β-o-thiogalactoside for 6 h at room temperature. Bacteria were harvested by centrifugation for 20 min at 2,100 g_{av}, and pellets were resuspended in solubilization buffer [PBS, 0.5 mg/mL lysozyme, 1 mM PMSF, DNase I, and an EDTA-free protease inhibitor mixture (Roche)]. Cells were broken by sonication, and insoluble material was removed by centrifugation for 30 min at 7,000 g_{av} and 4°C. Proteins were affinity-purified using glutathione Sepharose bead (Thermo Fisher) incubation overnight at 4°C, followed by TEV protease (Invitrogen) cleavage overnight at room temperature. His-tagged TEV protease was removed by incubation with Ni-NTA (Qiagen) overnight at 4°C. Protein concentrations were assessed using the bicinchoninic acid method according to the manufacturer's protocol (Thermo Scientific). Recombinant αSyn was subjected to aggregation as previously described (Burré et al., 2015).

Liposome binding assay

Liposomes of 30 nm diameter were prepared by sonication as previously described (Burré et al., 2010). Liposomes of 100 nm diameter were obtained through extrusion (Avanti Polar Lipids). For lipid-binding assays, a mixture of lipids (all Avanti Polar Lipids) in chloroform were dried in a glass vial under a nitrogen stream. Residual chloroform was removed by lyophilization for 2 h. Small unilamellar vesicles were formed by sonicating in PBS on ice. For lipid binding studies, synucleins were incubated with liposomes for 2 h at room temperature at a molar lipid/protein ratio of 400 or other ratios where indicated. For co-flotation experiments, αSyn, βSyn, and γSyn were added at a molar lipid/protein ratio of 800 each. Samples were then subjected to a liposome flotation assay (Burré et al., 2010).

FRET experiments

100 μM GST-fusion protein of αSyn, βSyn, or γSyn containing a cysteine (positions 8 and 96 for αSyn and γSyn, positions 8 and 85 for βSyn) were captured on glutathione beads (Thermo Fisher). GST-synucleins were reduced with 1 mM DTT for 20 min at 4°C. Beads

were washed four times with PBS containing protease inhibitors and proteins were labeled with 2 mM Alexa 488 C5 maleimide or Alexa 546 C5 maleimide (Thermo Fisher) overnight at 4°C in the dark. Beads were washed four times with PBS to remove residual unbound dye, and synuclein was eluted from the GST moiety using TEV protease overnight at room temperature. His-tagged TEV protease was removed using Ni-NTA agarose (Qiagen). Labeling efficiency was calculated using the following formula:

$$\text{Moles dye per mole protein} = \frac{A_{max} \text{ of labeled protein}}{\varepsilon \times \text{protein concentration(M)}} \times \text{dilution factor}$$

with

$$\text{Protein concentration(M)} = \frac{A_{280} - (A_{max} \times CF)}{\varepsilon'} \times \text{dilution factor}$$

(ε = molar extinction coefficient of the protein ($\varepsilon^{\alpha Syn}$ = 5960 $cm^{-1}M^{-1}$, $\varepsilon^{\beta Syn}$ = 5960 $cm^{-1}M^{-1}$, $\varepsilon^{\gamma Syn}$ = 1490 $cm^{-1}M^{-1}$); ε' = molar extinction coefficient of the fluorescent dye (Alexa Fluor 488 = 72,000 $cm^{-1}M^{-1}$, Alexa Fluor 546 = 93,000 $cm^{-1}M^{-1}$); A_{max} = absorbance of the dye molecule at 488 nm for Alexa 488 labeled synucleins or at 546 nm for Alexa 546 labeled synucleins; CF = correction factor that adjusts for the amount of absorbance at 280 nm caused by the respective dye (Alexa Fluor 488 = 0.11, Alexa Fluor 546 = 0.12)). For FRET experiments on liposomes, 2.5 μg of Alexa 488-labeled donor synuclein and 2.5 μg of Alexa 546-labeled acceptor synuclein were incubated with or without 100 μg of liposomes in 100 μL of PBS for 2 h at room temperature in the dark. For FRET experiments on immunoisolated synaptic vesicles, 50 μg of synaptic vesicles were captured on magnetic beads using an antibody to SV2 (Burré et al., 2006, 2007) and were incubated with 175 nM donor synuclein plus 175 nM unlabeled synuclein, 175 nM acceptor synuclein plus 175 nM unlabeled synuclein, or 175 nM donor plus 175 nM acceptor synuclein for 1 h at 4°C. Beads were washed three times with PBS. Emission spectra were measured using a Synergy H1 plate reader (BioTek; excitation: 490 nm; emission: 500–650 nm). FRET signals were measured using the following formula:

$$\text{FRET} = \frac{R_{D+A(-A \text{ only})}}{R_D}$$

with

$$R_{D+A(-A \text{ only})} = D + A\ (-A \text{ only}) \frac{573 \text{ nm}}{519 \text{ nm}}$$

and

$$R_D = D \frac{573\ nm}{519\ nm}$$

Circular dichroism spectroscopy

Circular dichroism (CD) spectra were measured on an AVIV 62 DS spectrometer equipped with a sample temperature controller. Far-UV CD spectra were monitored from 190 to 300 nm using final protein concentrations of 50 μM and 0.1 mM–15 mM small unilamellar vesicles (composition: 70% phosphatidylcholine, 30% phosphatidylserine; diameter: ~30 nm) with a path length of 0.2 mm, response time of 1 s, and scan speed of 50 nm/min. Each scan was repeated three times.

Immunocytochemistry

Cells were washed twice with phosphate-buffered saline (PBS) containing 1 mM $MgCl_2$ and were fixed with 4% paraformaldehyde in PBS for 20 min at room temperature. Cells were washed twice with PBS and permeabilized with 0.1% Triton X-100 in PBS for 5 min at RT. After washing twice with PBS, cells were blocked for 20 min with 5% bovine serum albumin (BSA) in PBS. Primary antibody was added in 1% BSA in PBS over night at 4°C. The next day, cells were washed twice in PBS, blocked for 20 min in 5% BSA in PBS and incubated with Alexa405-, Alexa488-, or Alexa555-coupled secondary antibody and DAPI in 1% BSA in PBS for 1 h at RT in the dark. Cells were washed twice with PBS and were mounted using Fluoromount-G. Cells were imaged on an Eclipse 80i upright fluorescence microscope (Nikon). For titration experiments in Figures 4 and S7, 5 μL of 40x concentrated virus expressing αSyn was added in addition to 0 μL, 0.2 μL, 0.5 μL, 1 μL, 2 μL, or 5 μL of 40× concentrated lentivirus expressing αSyn, βSyn, or γSyn (for synapsin co-stainings) or 0 μL, 1 μL, or 5 μL of 40× concentrated lentivirus expressing βSyn or γSyn (for SV2A co-stainings)

QUANTIFICATION AND STATISTICAL ANALYSIS

Sample sizes were chosen based on preliminary experiments or similar studies performed in the past. For quantification of immunoblots, a minimum of three independent experiments were performed. For quantification of immunofluorescence microscopy images, images were recorded under the same microscope settings (objective lens and illumination intensity) to ensure reliable quantification across samples and images. In addition, images of each biological replicate were taken and analyzed on the same day. Merged images were created using Photoshop (Adobe), and were analyzed using ImageJ (NIH) or Image Studio (LI-COR). No samples or

animals were excluded from the analysis, and quantifications were performed blindly. All data are presented as the mean ± SEM, and represent a minimum of three independent experiments. Statistical parameters, including statistical analysis, significance, and n value are reported in each figure legend. Statistical analyses were performed using Prism 8 Software (GraphPad). For statistical comparison of two groups, either two-tailed Student's t test or two-way ANOVA followed by Bonferroni post hoc test was performed, as indicated in the figure legends. A value of $p < 0.05$ was considered statistically significant. All statistical details of experiments can be found in the figure legends.